Ocean Engineering 278 (2023) 114236

Contents lists available at ScienceDirect

Ocean Engineering

journal homepage: www.elsevier.com/locate/oceaneng

Numerical analysis of fishtailing motion, buoy kissing and pullback force in a catenary anchor leg mooring (CALM) moored tanker system

Xuanze Ju[a,**], Chiemela Victor Amaechi[b,c,d,*], Baohui Dong[a], Xianwu Meng[a], Junji Li[a]

[a] *Offshore Oil Engineering Co., Ltd., Engineering Company, Tianjin, 300451, China*
[b] *School of Engineering, Lancaster University, Bailrigg, Lancaster, LA1 4YR, UK*
[c] *Standards Organisation of Nigeria (SON), 52 Lome Crescent, Wuse Zone 7, Abuja, 900287, Nigeria*
[d] *Institute of Sustainable Energy, Universiti Tenaga Nasional (The National Energy University), Jalan IKRAM-UNITEN, Kajang, 43000, Selangor, Malaysia*

ARTICLE INFO

Handling Editor: Prof. A.I. Incecik

Keywords:
Offshore floating structure
Catenary anchor leg mooring
Tanker
Hydrodynamic
Mooring
Floating buoy
Fishtailing

ABSTRACT

The catenary anchor leg mooring (CALM) sys tem is one of the most complex hydrodynamic systems in terms of hydrodynamic theory. This complexity comes from a large amount of interaction between the buoy, its mooring legs, hawsers, and the moored tanker. A dynamic simulation analysis of a CALM moored tanker system is carried out in this research. A double spring hydrodynamic response system model composed of "Anchoring-Buoy" and "Hawser-Tanker" established for the CALM system in the given environmental conditions with the method of time domain coupling simulation, correlation, and comprehensive analysis simulations of the fishtailing motion, buoy kissing, hawser capacity, and pullback force. A numerical analysis shows that without pullback force, fishtailing occurs often. A pullback force of 800 kN in line with the tanker's centerline effectively reduces the yaw motion and preserves a safe distance between the tanker and the buoy, so fishtailing occurs less often, and buoy kissing does not occur. Thus, the pullback force of 800 kN represents astern propulsion and a pullback tug, as it significantly improves the behavior of the moored tanker in relation to the buoy. Therefore, it is recommended that a tug is always present while a tanker is moored to the CALM system.

1. Introduction

The transport of petroleum products to export destinations is conducted either by pipeline or in oil terminals. Onshore and offshore terminals are the common types of oil terminals. However, due to geographical and economic conditions, the number of ports available for the construction of oil terminals is limited, resulting in the increase of secondary transport costs, the detention of oil tankers arriving at a port, and other issues. Therefore, it is necessary to study other types of offshore oil loading/offloading facilities to cooperate with or replace oil terminals. There are various mooring forms like the Single Point Mooring (SPM), Conventional Multi-Buoy Mooring (CBM/MBM), and Single Anchor Loading Mooring (SALM) systems. The most common type of offshore terminal is the Catenary Anchor Leg Mooring (CALM) system, which is a form of Single Point Mooring (SPM) (Shell DEP 37, 2011). However, each configuration is designated for connection to tankers/ships as a unique solution for offloading and loading hoses. A typical schematic for the CALM system is shown in Fig. 1. Since the CALM system was introduced in 1958 (Maari, 1985), it has operated 85% of the world's 700 oil terminals (Cheng and Wang, 2017; Lv et al., 2018), with extensive operations in Southeast Asia, the Middle East, and West Africa. In particular, deepwater offloading CALM buoys are being extensively used in West Africa to allow the efficient loading of spread-moored FPSO (Ryu et al., 2006), and the maximum applied water depth has reached 1435 m (Agbami oil field, Nigeria) (Hollister and Spokes, 2004). With the progress of China's offshore engineering technology, attention has also been paid to the CALM system, including the overall design of the CALM system (Lv et al., 2018; Wu, 2004), mooring analysis (Zhou et al., 2020; Sun et al., 2014), submarine hose fatigue analysis (Amaechi et al., 2019), system model testing (Fang and Xu, 1989; Xu and Tong, 1994), and other technical aspects. In 2019, China's first CALM system assembly was successfully developed and delivered for project applications (Hengyi Brunei PMB petrochemical project, 2019). In addition, due to the high cost of construction and maintenance, complexity in berthing, and dredging issues in China, applications of the CALM system at Caofeidian port (Ji et al., 2014) and

* Corresponding author. School of Engineering, Lancaster University, Bailrigg, Lancaster, LA1 4YR, UK.
** Corresponding author.
E-mail addresses: sinoju@126.com (X. Ju), chiemelavic@gmail.com (C.V. Amaechi).

https://doi.org/10.1016/j.oceaneng.2023.114236
Received 17 September 2022; Received in revised form 26 February 2023; Accepted 16 March 2023
Available online 7 April 2023

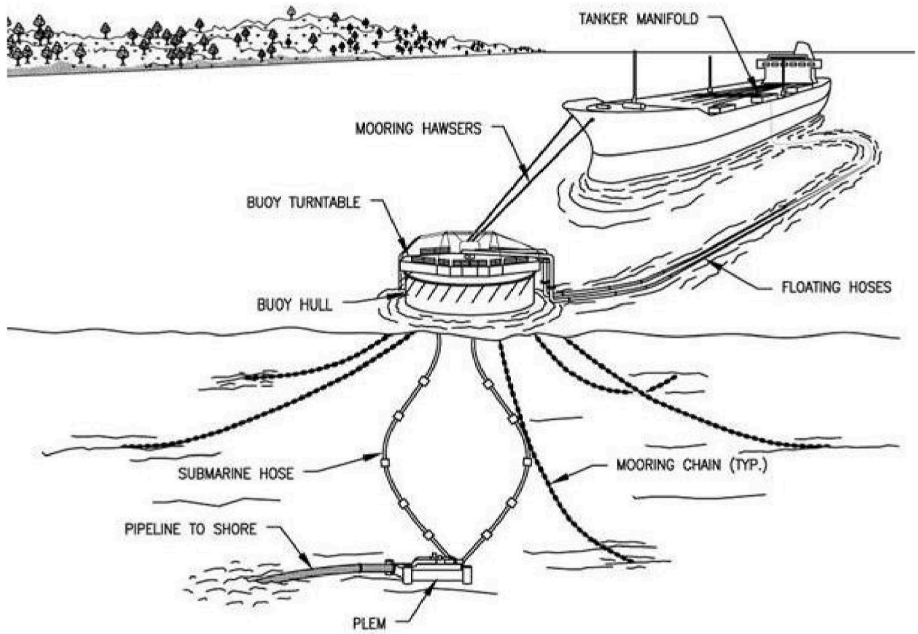

Fig. 1. Schematic of a typical catenary anchor leg mooring (CALM) system (Shell DEP 37, 2011). Permission was obtained to adapt, reuse and reproduce as it was also published in an open access publication. Publisher: Hindawi; Copyright year: 2022; Secondary Source: Ju et al., 2022a).

Dongying port (Liang et al., 2019) are also being considered.

In both scientific studies and actual offloading operations, a characteristic of the CALM system is that even in the absence of time variations in the environmental forces (e.g., in constant winds and currents), significant dynamic effects can occur, leading to extraordinarily large periodic horizontal motions, that is, fishtailing motion. As a result of this type of fishtailing motion, a tanker may drift toward a buoy and the tanker and buoy may collide. This is called buoy kissing. The large frequency motion of the tanker in the horizontal plane will cause the phenomenon of periodical tensioning–relaxation–tensioning of the CALM system's hawser. Studies have shown that the maximum hawser tension in this state will increase by more than 50% compared with that in the steady state, which is considered to be the main cause of a hawser's sudden breakage in the CALM system (Gu, 2006). Wichers. (1988) performed one of the earliest studies on a CALM moored tanker: a systematic numerical analysis of the CALM moored tanker system was conducted, and a detailed analysis was made of the environmental loads on the tanker, including its motion equation, potential flow load, and viscosity load. Based on this, a numerical model was established to predict the plane motion of a CALM moored tanker. Schellin T. E (Schellin, 2003). studied the mooring force characteristics and plane motion characteristics of a CALM moored tanker in steady flow. Mathieu Brotons et al. (Brotons and Jean, 2005) studied the yaw motion of a CALM moored tanker by means of numerical simulation and model testing. Ma S. and Kim M. H. et al. (Ma et al., 2009) investigated the calculation method of the low-frequency wave load of a CALM moored tanker in shallow water. Halliwell and Harris (1988) conducted a model test study on a CALM moored tanker and showed that fishtailing might also occur in the CALM moored tanker model in regular waves. Additionally, the fishtailing motion period was much larger than the wave period. The model test also showed that whether the tanker model has fishtailing motion has a high level of relationship with the combination of wave period and wave amplitude. Simos A. N. et al. (Simos et al., 2001a) conducted theoretical analysis and experimental evaluation of the fishtailing phenomenon in a single-point moored tanker and presented a rich dynamic scenario, limit cycle oscillations and chaotic response being possible situations. Not only the dynamic behavior of the system is difficult to be theoretically described but also its experimental evaluation is usually awkward. Sao Paulo (Simos et al., 2001a) also used numerical simulation and model testing to analyze the fishtailing motion of a CALM moored tanker. Huang Guiliang and Masayaka Fujino (Huang and Fujino, 1987) studied the plane motion characteristics of a CALM moored tanker under wind loads and current loads with a model test and a steady-equilibrium state eigenvalue method based on the maneuvering equation. Sun C. Q. et al. (Sun et al., 1988) investigated the motion response of a CALM moored tanker in a wave-facing state with a model test. Fang Huacan (Fang and Xu, 1989) and Xu Xingping (Xu and Tong, 1994) researched the causes of the six degrees of freedom motion of a CALM moored tanker by means of mathematical modeling and a model test. Yu Jianxing et al. (Yu et al., 2005) conducted a stress analysis of a CALM moored tanker with the combined effects of wind, waves, and currents. Ji C. Q. et al. (Ji, 2000) analyzed the motion response characteristics of a CALM moored tanker in wind, currents, and waves, and discussed the influence of the tanker's main parameters, load condition, and mooring system related to the tanker motion. Zhang X. M. et al. (Zhang and Li, 1988) also analyzed the motion of the CALM system with the combined action of wind, waves, and currents. Zhang L. et al. (Zhang et al., 2012) analyzed the hydrodynamic performance and motion characteristics of a CALM buoy and shuttle tanker during joint operations. In addition, numerical simulation in the time domain can be used to quantitatively calculate the fishtailing motion of a CALM moored tanker, while stability analysis can be used to qualitatively determine whether the fishtailing motion of a CALM moored tanker occurs. Zhou Nan (Zhou, 2018) carried out a fishtailing motion simulation analysis in a mooring analysis for the first CALM system project in China and proposed some engineering approaches for dealing with fishtailing motion. Ge S (Ge et al., 2022). and Li Y. Z. et al. (Li and Liu, 2019) conducted a numerical simulation and sensitivity analysis of the tanker fishtailing motion phenomenon based on the background of the CALM system of SINOPEC Maoming Petrochemical Company. This CALM system was recorded as the first application in China that considered this phenomenon (Cai, 2018).

It can be seen from the aforementioned studies, that compared with the current research methods on the motion characteristics of a CALM moored tanker, motion stability analysis can be used to judge whether a tanker can achieve stability in a stationary mooring position. It can also be used to calculate whether the moored floating structure will vibrate when the equilibrium mooring point is unstable. However, it is not enough to analyze the stability of the tanker's motion at the equilibrium mooring point. Asmara and Wibowo (2020) conducted an investigation on the safety analysis of mooring hawsers of an SPM system by using safety factors (S.F.) from motion simulations. Thus, the need for better understanding of CALM buoy motion under different perspectives by considering the hydrostatics, hydrodynamics and wave-current interaction (WCI) from both mathematical and numerical modelling (Asmara and Wibowo, 2020; Amaechi et al., 2021a, 2021b; Ju et al., 2022a; Yang and Chiang, 2022a; Edward and Dev, 2020). Developments made in this field are also depicted in studies presented on the stability of SPMs using mathematical modelling (Esmailzadeh and Goodarzi, 2001; Bernitsas and Papoulias, 1986), and the hydrodynamic performance due to the configuration of the marine hose (Brown and Elliot, 1987, 1988). Although the phenomenon of fishtailing motion of a CALM moored tanker was revealed in the previous study, the simulation model in the study only provided qualitative analysis and suggestions for the elimination of fishtailing motion, without quantitative analysis and calculation. The buoy kissing phenomenon has rarely been studied, though different safety considerations have been considered in selecting SPMs by various researchers (Asmara and Wibowo, 2020; Ziccardi and Robbins, 1970; Lu et al., 2018; Ju et al., 2022b; Lee and Kim, 2019; Hasanvand and Edalat, 2021a). The type of configuration deployed on floating buoys at oil terminals have been considered, such as the Chinese-lantern configuration and Lazy-S configuration with comparative designs on adaptable mooring systems like CALM, and SALM (Hasanvand and Edalat, 2020, 2021b, 2021c; Rutkowski, 2019a, 2019b; Pecher et al., 2014; Eedalat and Hasanvand, 2021). These designs are conducted using industry rules, such as DNV, ABS and OCIMF standards (ABS, 2022; DNVGL, 2015; DNVGL, 2020; OCIMF, 2009; OCIMF, 2015; OCIMF, 2018).

Therefore, in this research, a double spring hydrodynamic response system model is established that is composed of "Anchoring-Buoy" and "Hawser-Tanker" for a CALM system in the given environmental conditions. Using the method of time domain coupling simulation, correlation and comprehensive analysis simulations of the fishtailing motion, buoy kissing, hawser capacity, and pullback force are conducted. Additionally, the quantitative results of the pullback force required to avoid fishtailing motion and buoy kissing are obtained through simulation analysis. Section 1 introduces this research while Section 2 presents the methodology for the study. Section 3 presents the CALM characteristics while Section 4 presents the mooring motion criteria. Section 5 presents the results and discussion, while the concluding remarks drawn with some recommendations for future research are presented in Section 6.

2. Methodology

The CALM system generally has two states. The first state is the single floating structure's state whereby it is without a tanker connection, for which the engineering focus is on the survival conditions. The other state is that under the allowed operational environment conditions, the CALM system has a moored tanker to form a double floating structure state, which is considered an operational condition for engineering. Whether in survival conditions or operational conditions, the load of the system mainly includes the following.

a) Steady forces from wind, waves, and current
b) First-order wave exciting forces
c) Wave frequency buoy and tanker motions
d) Wave drift forces and low-frequency tanker motions
e) Coupled mooring–buoy–tanker dynamics
f) Mooring line dynamics

For the dynamic mooring analysis, the software program aNySIM was used. aNySIM is developed by MARIN (Maritime Research Institute Netherlands) (MARIN, 2022; van den Berg and Pauw, 2018). aNySIM comprises a time domain simulation of the dynamic behaviour of a tanker coupled to the buoy subjected to wind, waves and current. It allows for the calculation of the motions of the ship and buoy (including weathervaning) and mooring forces (i.e. hawser and chain forces). aNySIM solves the equations of motion of the vessel in the time domain, so that nonlinear behaviour of mooring lines, anchor chains and drift forces are taken into account. aNySIM is a software for simulating offshore structures, by computing the motions of the vessels that result from non-linear hydrodynamic and mechanical loading, as seen in various validated studies (MARIN, 2022; van den Berg and Pauw, 2018; Gueydon et al., 2014; Gueydon et al., 2013; Gueydon, 2016; Weller and Gueydon, 2012).

Following the industry specifications on the design of SPM systems, it is pertinent to give the theoretical basis for simplifying the anchor chains and nylon cables to non-linear springs in this study. Earlier mathematical models have considered mooring lines and marine hoses using line theory models (Amaechi et al., 2019, 2021b), and other theoretical modelling approaches. Some other studies were based on different mooring systems with material considerations (Asmara and Wibowo, 2020; Amaechi et al., 2021a, 2021b; Ju et al., 2022a; Yang and Chiang, 2022a; Edward and Dev, 2020). Some authors made onward strides towards SPM development using theoretical models based on stability designs (Ge et al., 2022; Esmailzadeh and Goodarzi, 2001; Bernitsas and Papoulias, 1986; Brown and Elliot, 1987, 1988) while others presented comparative studies using CALM against SALM (Rutkowski, 2019a, 2019b; Pecher et al., 2014; Eedalat and Hasanvand, 2021; Hasanvand and Edalat, 2021b, 2021c). Thus, the justification on the simplification approach in this study utilized for the anchor chains and nylon cables to non-linear springs make the system run in validated software, as referenced in the theory documentations (Wichers., 1988, 2013; Bai and Bai, 2005; Berteaux, 1976).

Simplification in theory, is considered based on different factors, such as the system's elements, the composition of the materials, the static model, the dynamic model, the computational resources in terms of running time, and number of equations that need to be decomposed. Recent studies that applied simplifications include Gueydon S et al. (van den Berg and Pauw, 2018; Gueydon et al., 2014; Gueydon et al., 2013; Gueydon, 2016; Weller and Gueydon, 2012) which applied simplification in modelling the mooring systems for OC4-DeepCwind semi-submersible FOWT (floating offshore wind turbine) using aNySIM with other codes like FAST while Jin et al. (2022) which applied the Hamiltom variational principle, Newton's law and Morison formula for the design of the buoy-mooring for the SPMs. Each study has its design objective, however more industry problems exist, which are solved in recent studies providing solutions on failure analysis of mooring lines, using various approaches (Burmester et al., 2020; Eskilsson and Palm, 2022; Yu et al., 2023; Yu et al., 2022; Ja'e et al., 2022; Yang and Chiang, 2022b). In the same vein, aNySIM was applied on this present study for model simplification, as it saves time on the computational resources which will be discussed in subsequent sections. This study is comprised of a time domain simulation of the dynamic behaviour of a tanker coupled to the buoy subjected to wind, waves and current.

Similar to other types of mooring systems, after the main parameters of the CALM system are determined initially by the scheme design, a mooring analysis is carried out, and the results are used as the basis for the scheme verification and further engineering. Currently, the quasi-static method is often used to execute the mooring analysis in the preliminary engineering stage. The quasi-static method ignores the vertical motion and fluid change of the floating structure, considers the static drift of the floating structure in the direction of the waves and the motion effect caused by the wave dynamic load as well as the linear superposition of the two parts of the motion, and calculates the maximum mooring offset of the floating structure. For the soft yoke or turret mooring system, only one floating structure motion of the moored vessel coupled with mooring needs to be considered. The reason is that the mooring assembly is fixed at a certain point or moves synchronously

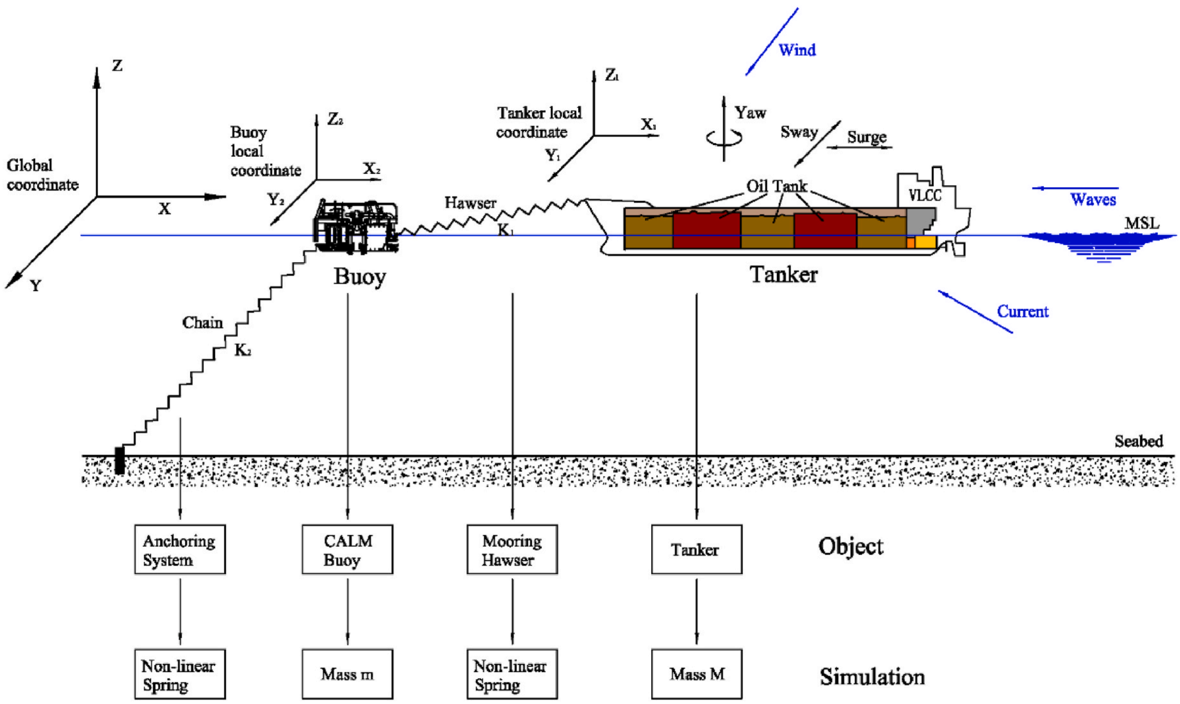

Fig. 2. Dual-spring hydrodynamic response model of the CALM moored tanker system.

with the moored vessel. In contrast, the CALM system is characterized by two floating structures - the moored tanker and the CALM buoy, which are connected and interact with each other. The tanker is connected with the CALM buoy by a nylon hawser, and the buoy is connected with a seabed anchor by a mooring anchor chain. When the tanker is moored on the CALM buoy and subjected to the external forces from wind, waves, and currents, the elastic response of the system is generated. Therefore, the whole system can establish a double spring hydrodynamic response system composed of "Anchoring-Buoy" and "Hawser-Tanker", as shown in Fig. 2.

2.1. Static stability analysis model

The purpose of the static stability analysis is to determine the static equilibrium position of the double floating system and calculate the equilibrium position of the coupling connected by the mooring system under specific environmental conditions. The coordinate axes system is defined as shown in Fig. 2. The reference axis of the global coordinate system is Oxyz, the origin is at the mean sea level (MSL), and the z axis is vertically upward. The local coordinates of the CALM buoy and tanker are $G_iX_iY_iZ_i(i = 1,2)$, where $i = 1$ and 2 indicate the tanker and the CALM buoy, respectively. The initial calculation of the floating structure position and direction of the CALM system can be expressed by vectors, as follows:

ADDIN CNKISM.UserStyle$$X^{(0)} = \begin{pmatrix} X_{g1}^{(0)}, Y_{g1}^{(0)}, Z_{g1}^{(0)}, \theta_{11}^{(0)}, \theta_{21}^{(0)}, \theta_{31}^{(0)}, \dots, \\ X_{gN}^{(0)}, Y_{gN}^{(0)}, Z_{gN}^{(0)}, \theta_{1N}^{(0)}, \theta_{2N}^{(0)}, \theta_{3N}^{(0)} \end{pmatrix} \tag{1}$$

where, $X_{gj}^{(0)}, Y_{gj}^{(0)}, Z_{gj}^{(0)}$ represents the position of the j weight center of the floating structure relative to the global coordinate system, $\theta_{1j}^{(0)}, \theta_{2j}^{(0)}, \theta_{3j}^{(0)}$ represents the rotation angle in the direction of the j floating structure, and the superscript represents the iterative step.

Then the new position $X^{(m)}$ of the floating structure is given in the m iteration:

$$X^{(m)} = K^{-1}\left(X^{(m-1)}\right)F\left(X^{(m-1)}\right) + X^{(m-1)} \tag{2}$$

where K is the stiffness matrix and F is the total external force vector. The process is repeated until n iterations, $\left|(X^{(n)}) - X^{(n-1)}\right|$ less than the prescribed limit of convergence.

2.2. Dynamic stability analysis model

Given that the static equilibrium position of the system is X_B, the motion equation of the system regarding its equilibrium position can be expressed in the Hamiltonian form:

$$\begin{bmatrix} M_t & 0 \\ 0 & M_t \end{bmatrix}\begin{Bmatrix} \dot{V} \\ U \end{Bmatrix} + \begin{bmatrix} B & K \\ -M_t & 0 \end{bmatrix}\begin{Bmatrix} V \\ U \end{Bmatrix} = \begin{Bmatrix} F \\ 0 \end{Bmatrix} \tag{3}$$

where M_t is the total mass matrix including the floating structural mass and additional mass, and B is the damping matrix.

The velocity vector $V = U$ can be expressed in another form:

$$\begin{Bmatrix} V \\ U \end{Bmatrix} = \begin{Bmatrix} V_0 \\ U_0 \end{Bmatrix} e^{\lambda t} \tag{4}$$

$$\lambda = f + i\omega_n \tag{5}$$

Then the eigenvalues of Equation (3) can be given by the following formula:

$$\begin{bmatrix} M_t^{-1}C & M_t^{-1}K \\ -I & 0 \end{bmatrix}\begin{Bmatrix} V_0 \\ U_0 \end{Bmatrix} + \lambda\begin{Bmatrix} V_0 \\ U_0 \end{Bmatrix} = \begin{Bmatrix} 0 \\ 0 \end{Bmatrix} \tag{6}$$

where I is the unit vector matrix. The system characteristic values given by Equations (5) and (6) can represent the motion state of the double floating body system. When $f < 0$ and always, the system is stable. When $f > 0$ and $\omega_n = 0$, the system is unstable. When $f > 0$ and $\omega_n \neq 0$, there is fishtailing motion.

2.3. Time-domain low-frequency motion analysis model

In the operational conditions, the analysis procedure consists of the determination of the low-frequency motion of a moored tanker with the effect of irregular waves, winds, and currents, followed by a super-

Table 1
Tanker particulars.

Description	Symbol	Unit	VLCC (Very Large Crude Carrier)			Suezmax	
			Ballasted	Partly loaded	Loaded	Ballasted	Loaded
Deadweight	DWT	t	320,000			160,000	
Displacement	/	m^3	146,230	~249,300	356,658	73,823	180,057
Mass	/	t	149,886	~255,500	365,575	75,669	184,558
displacement of loaded condition	/	%	~40%	~70%	100%	~40%	100%
Length overall	L_{OA}	m	355			276	
Length between perpendiculars	L_{PP}	m	320			264	
Breadth	B	m	60			48	
Moulded depth	D	m	30.5			23	
Draught	T	m	9.5	16	22.5	7.1	17.4
Side wind area	A_S	m^2	8685	6378	4070	4966	2124
Front wind area	A_F	m^2	2173	1783	1393	1257	762

Table 2
CALM buoy particulars.

Description	Unit	Value
Height	m	5.3
Diameter	m	12.5
Draft	m	3.7
Weight	t	378
Vertical position of hawser wrt keel	m	8
Distance position of anchor line attachments from centre buoy	m	6
Vertical position of anchor line attachments wrt keel	m	0

position of the wave frequency motions. Due to the large displacement of the tanker and the flexibility of the CALM system, the low-frequency motion of the tanker is significantly influenced by the current load, the drag force, and the responses of the floating structure as well as the mooring lines' coupling. In this model, the mooring lines are coupled with the vessel responses. The low-frequency tanker's motion for a tanker moored to a CALM buoy can be obtained with time domain simulations, which solve the equation of motion at each time step in the following convolution integral matrix form:

$$\{\boldsymbol{M}+M_A\}\ddot{\boldsymbol{x}}(t)+\boldsymbol{B}\dot{\boldsymbol{x}}(t)+\boldsymbol{K}\boldsymbol{x}(t)+\int_0^t h(t-\tau)\ddot{x}(\tau)d\tau=\boldsymbol{F}^{(1)}(t)+\boldsymbol{F}^{(2)}(t)+\boldsymbol{F}_c(t)+\boldsymbol{F}_w(t)+\boldsymbol{F}_b(t)+\boldsymbol{F}_m(t) \tag{7}$$

where M is the mass matrix of the floating body structure, M_A is the added mass matrix of the floating structure , B is the damping matrix including linear radiative damping, K is the total stiffness matrix, $\boldsymbol{F}^{(1)}(t)$ and $\boldsymbol{F}^{(2)}(t)$ represent the wave forces of order 1 and order 2, respectively. $\boldsymbol{F}_c(t)$ is the current force, $\boldsymbol{F}_w(t)$ represents the wind force, $\boldsymbol{F}_b(t)$ is the nonlinear rolling damping force, and $\boldsymbol{F}_m(t)$ is the mooring force.

The goal of the dynamic mooring analysis (DMA), based on the above model, is to study the motion of the CALM buoy under the influence of the double spring system, which should take reasonable elasticity and proper rigidity into account. The fishtailing and buoy kissing are assessed according to the DMA, which comprises a time domain simulation of the dynamic behavior of a tanker coupled to the buoy subjected to wind, waves, and currents. This allows for the calculation of the motions of the ship and buoy (including weathervaning) and mooring forces (i.e., hawser and chain forces) so that the nonlinear behaviors of the mooring lines, anchor chains, and drift forces are taken into account. The simulation length is 4 hours (including 1 hour of initialization).

3. CALM system characteristics

3.1. Tanker characteristics

The tanker characteristics of the VLCC and Suezmax tankers are depicted in Table 1。

Table 3
Anchor chain characteristics.

Description	Unit	Value
Number of anchor chains	–	6
Arrangement wrt buoy	°	60
Length	m	354.7
Diameter	mm	90
Submerged weight	N/m	1382
Weight in air	kg/m	162
Grade/Type	–	R4S/Studless
Breaking Strength	kN	9062
Stiffness (EA)	kN	7.0×10^5
Pretension	kN	100

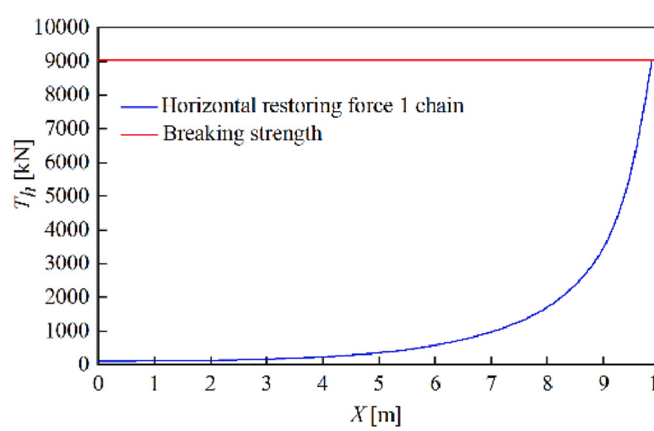

Fig. 3. Horizontal restoring force in one chain due to the horizontal displacement buoy in line with chain.

3.2. Buoy details

The following CALM buoy characteristics are used in the DMA.

3.3. Anchor chain characteristics

The following anchor chain characteristics are used in the DMA, refer to Table 3.

Fig. 3 shows the relation between the horizontal displacement of the buoy in line with the chain and the horizontal restoring force of the chain. (X [m] vs T_h [kN], in which X is the horizontal displacement of the buoy in line with chain and T_h is the horizontal force generated by one chain pulling the buoy back).

3.4. Hawser characteristics

The following hawser line characteristics are used in the DMA, refer

Table 4
Hawser characteristics.

Description	Unit	Value
Material type	–	Double braid nylon
Rope construction	–	Single line (refer to Fig. 4)
Unstretched length	m	70
Number of legs	–	2
Circumference	Inch	15
Diameter of 1 leg	Mm	121
Breaking strength 1 leg	kN	3756

to Table 4.

While Fig. 4 shows the sketch of a single line considered in the rope construction, Fig. 5 shows the load-elongation curves for different line materials. In the DMA, the load-elongation curve for nylon has been used. The load-elongation curves of both legs are calculated for the line's length and the breaking strength (see Fig. 6). Mooring line terminates at the mooring bit on the vessel. This is taken into consideration for the design of the mooring line's length.

3.5. Wind and current coefficients

The motion characteristics used in this investigation includes wind, waves and current. The details on the wind and current coefficient for both vessels is presented in Appendix A-C.

3.6. Environmental conditions

The behaviour of the moored tankers to the CALM buoy is determined by the unique combination of wind, waves and current. The mooring system is weathervaning (i.e. the process by which the floating structure passively varies its heading in response to time-varying environmental actions, such as wind). Note that during weathervaning, the tanker can be allowed to spin along the direction of wind freely so that no breakage/damage to the mooring system occurs due to the force of the moving wind. In this study, the tanker was designed to find a mean heading, which depends on the wind, wave and current conditions. The tanker often shows an oscillatory response induced by wind, waves and current due to the instable character of the mooring system. To limit the number of simulations, the environmental conditions for the DMA are sorted in classes, identifying: wave height, period and direction, wind speed and direction and current speed and direction. Each class has a certain probability of occurrence, calculated as the number of times that a certain class occurs in the data set divided by the total length of the data set. Table 5 depicts the range of classes of the wind and current speed and directions and the wave height, period and direction.

The above-mentioned classes lead to a total of 3576 unique combinations. To limit the number of simulations to a manageable amount, the number of unique combinations of wind, waves and current included in the DMA is 1200. For this purpose, the 3576 unique combinations of wind, wave and current are sorted from high probability to low. Then Fig. shows that the first 100 simulations already cover 61% probability of occurrence. For increasing run numbers, the contribution to the total probability of occurrence quickly reduces (see Fig. 7), whereas the accumulated probability of occurrence slowly increases (see Fig. 8). Since the simulations take time, it has been decided not to include the last 2376 combinations since they only cover 3.7% probability of occurrence. The sensitivity of the overall operational downtime to not

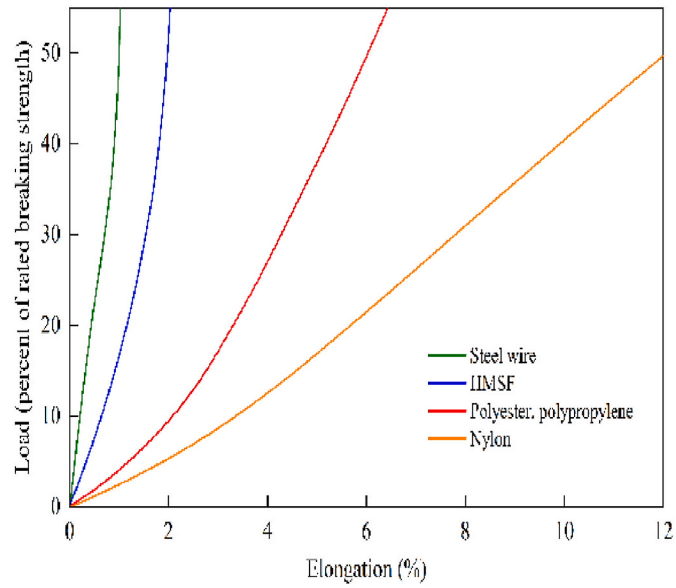

Fig. 5. Load-elongation curves mooring lines (OCIMF, 2018).

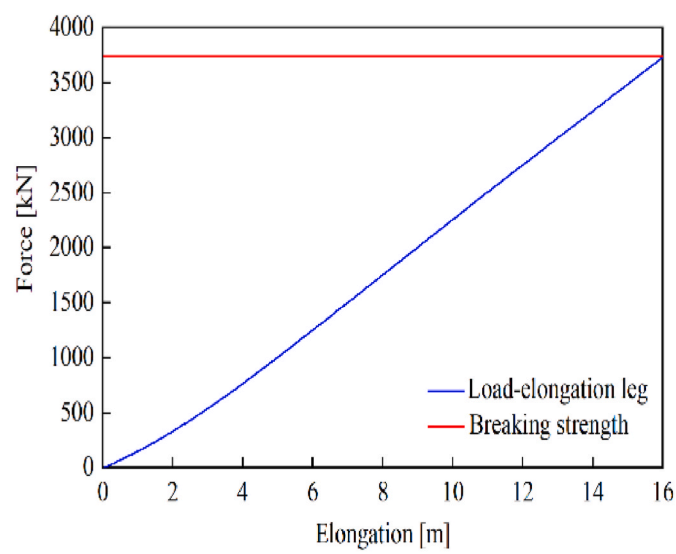

Fig. 6. Load-elongation curve one leg in hawser (OCIMF, 2018).

Table 5
Range of environmental conditions and their classes.

Description	Waves			Wind		Current	
Parameter	H_{m0} (m)	T_p (s)	Dir (° N)	U_w (m/s)	Dir (° N)	U_c (m/s)	Dir (° N)
Minimum	0	0	0	0	0	0	0
Maximum	4.5	22	337.5	20	315	0.8	337.5
Class width	0.5	2	22.5	5	22.5	0.2	22.5

Fig. 4. Sketch of a single line (OCIMF, 2018).

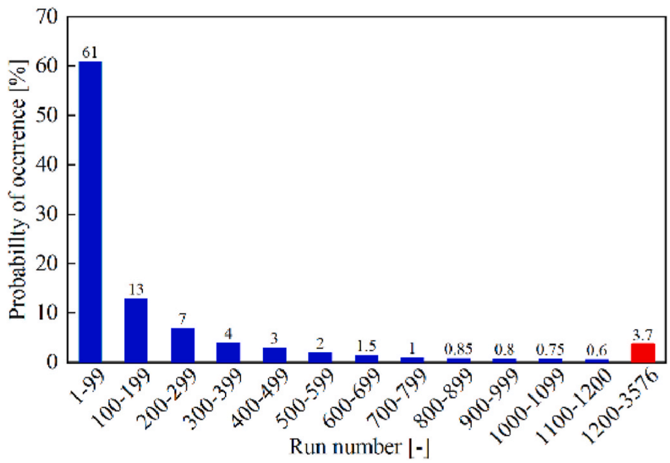

Fig. 7. Relation run numbers and probability of occurrence.

knowing whether the mooring is safe or not for these environmental conditions is addressed in the operational downtime assessment.

4. Mooring motion criteria

4.1. Motion criteria

To identify whether fishtailing and/or buoy kissing occurs two motion criteria have been defined.

1. Fishtailing occurs when the yaw motion exceeds ±20° (i.e. 20°<yaw<20°)
2. Buoy kissing occurs when the tanker collides with the buoy; the minimum safe distance is set to 10 m (radius buoy + ~3 m margin)

For a tanker moored to a CALM system, horizontal motions (sway and yaw) with slowly varying large amplitude could occur in specific wind, wave and current conditions. These motions could in turn lead to large peak loads in the bow hawser. In this paper, it is important to define some key terms used in this study. Fishtailing is defined as large yaw motions (>±20°). Buoy kissing is the relative distance between the tanker (bow) and the buoy. The relative distance is calculated, as it includes the horizontal motions (i.e. surge, sway and yaw) of the buoy and the tanker. Both fishtailing and buoy kissing are not taken into account

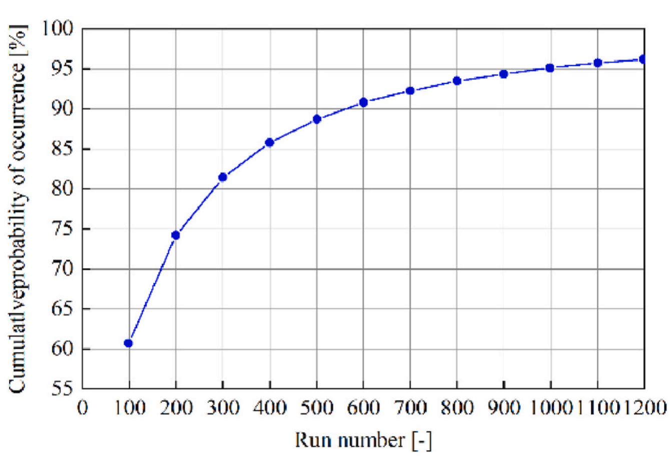

Fig. 8. Run numbers and cumulative probability of occurrence.

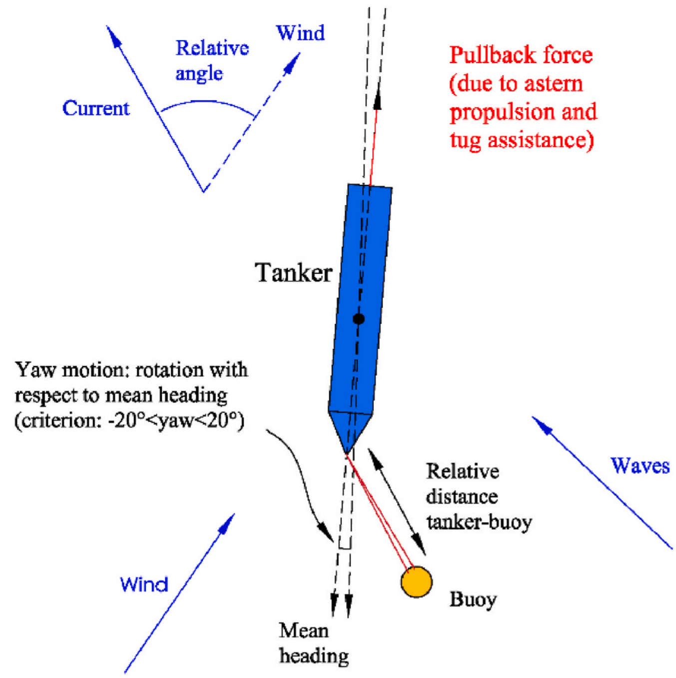

Fig. 9. Definition's directions and angles.

in the calculation of downtime. Fishtailing on its own is not dangerous and the results have shown that if a pullback force is applied, buoy kissing does not occur. This paper shows the relation between the environmental conditions and the tanker motions, in particular on the occurrence of fishtailing and buoy kissing. It also states that if astern (i.e., near or toward the stern of a ship or facing reverse/backwards), the propulsion and/or a pullback tug is sufficient to avoid fishtailing and buoy kissing.

4.2. Definition-directions, angles and yaw motion

In principle, fishtailing phenomenon sometimes occurs due to larger yaw motion of the SPM vessel, thereby influencing the hawser's mooring force, which may suddenly increase and exceed its breaking load (Huo et al., 2018). There are various extensive studies identified in respect to the fishtailing oscillations, which were all geared towards ensuring the safety of an SPM system in its mooring system design (Huo et al., 2018; Aghamohammadi and Thompson, 1990; Simos et al., 2001b; Tannuri et al., 2001; Hollyhead et al., 2017; Zhang et al., 2021). However, there is none that covered both fishtailing and buoy kissing – thus the need for this study.

The behaviour of the moored tankers depends on the environmental conditions, not only on the significant wave height, wind and current speed, but also on their relative directions. For fishtailing the relative direction between wind and current is important. Fishtailing is more likely to occur when the relative angle between wind and current is large. This angle has been defined as "relative angle" in the figures presented in this paper. The yaw motion is the rotation around the mean heading of the tanker. The maximum yaw amplitude in the time-series (positive or absolute negative, whichever is largest) is used to address whether or not fishtailing occurs. As per the previous Fig. 2, the following Fig. 9 further shows a sketch of the wind, wave and current directions, the relative direction and the yaw motion relevant for the interpretation of the plots. The description presented on the Methodology in the Section 1, shows that the illustration in Fig. 9 is connected with the illustration in Fig. 2, which is a dual-spring hydrodynamic

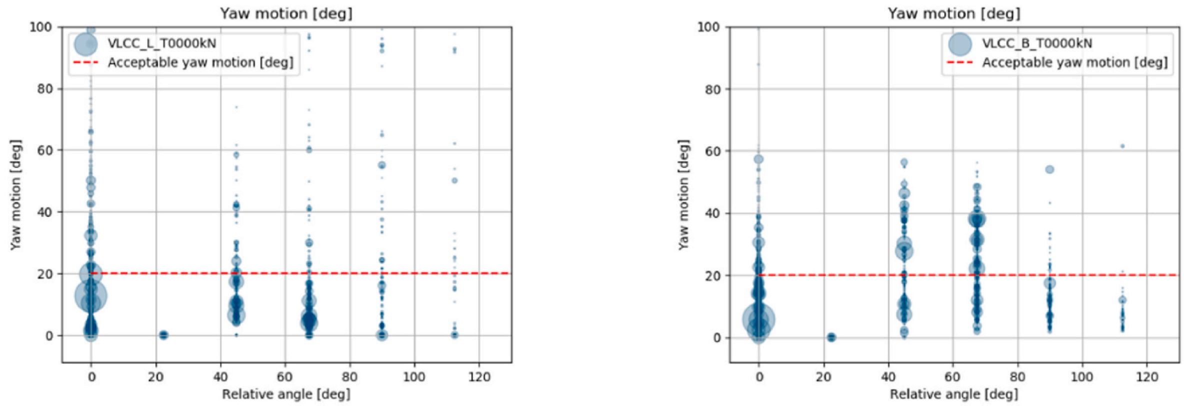

(a) VLCC loaded

(b) VLCC ballasted

Fig. 10. Effect of the relative angle between wind and current direction on the yaw motion of the VLCC in case no pullback force is applied.

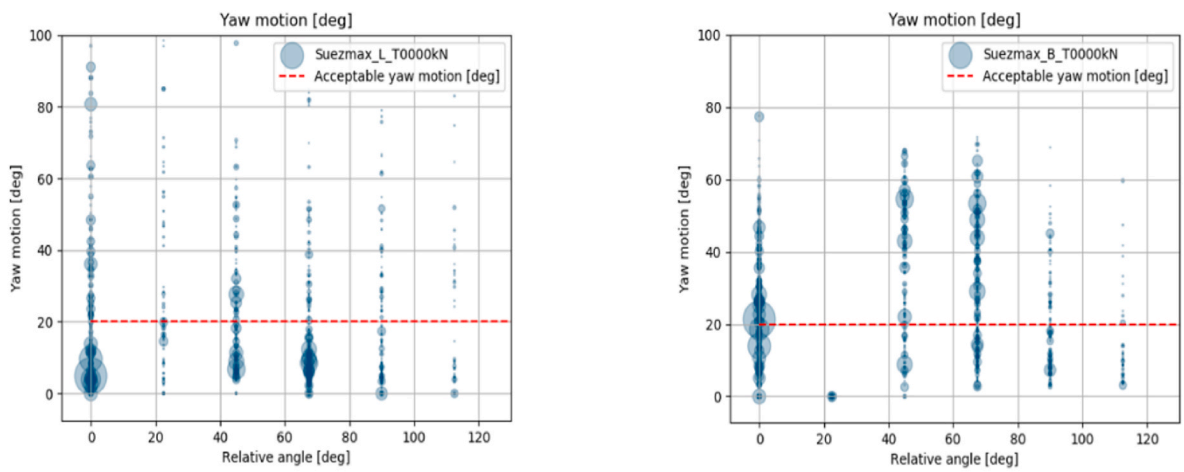

(a) Suezmax loaded

(b) Suezmax ballasted

Fig. 11. Effect of the relative angle between wind and current direction on the yaw motion for Suezmax in case no pullback force is applied.

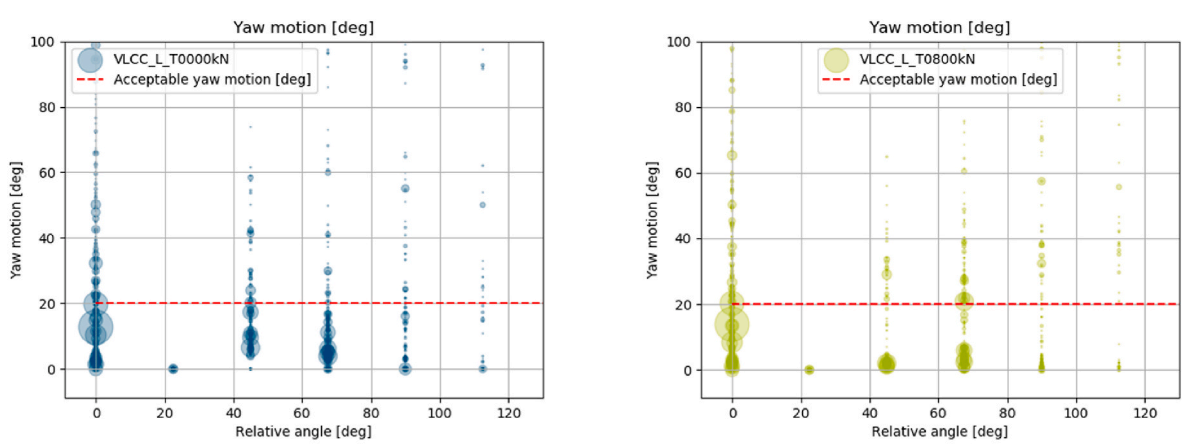

(a) VLCC loaded without pullback force

(b) VLCC loaded with pullback force

Fig. 12. Effect pullback force on yaw motion for VLCC loaded.

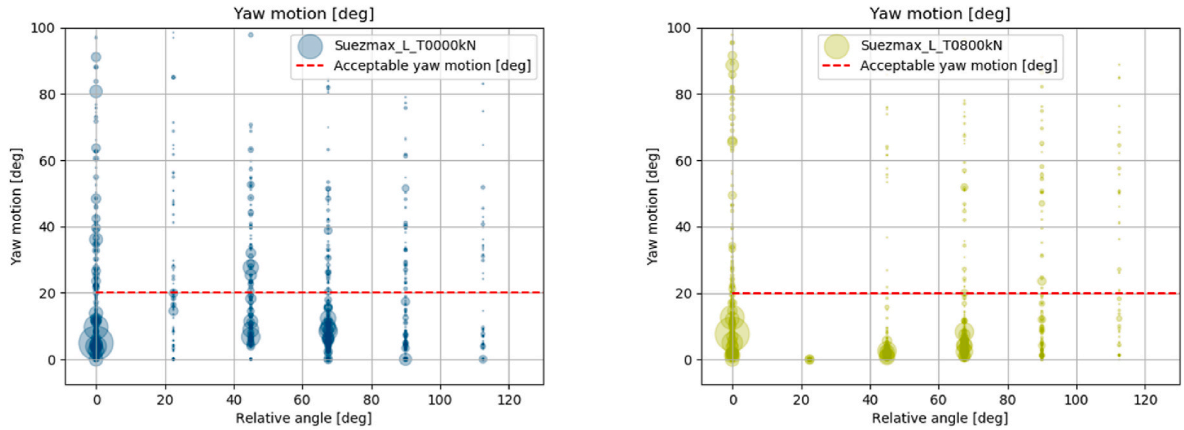

(a) Suezmax loaded without pullback force

(b) Suezmax loaded with pullback force

Fig. 13. Effect pullback force on yaw motion for Suezmax loaded.

response model of the CALM moored tanker system. On the other hand, the main purpose for including Fig. 9 here is to illustrate that the behaviour of the moored tankers depends on the environmental conditions, not only on the significant wave height, wind and current speed, but also on their relative directions.

5. Results and discussion

5.1. Without pullback force fishtailing occurs often

Without pullback force, fishtailing occurs often. The maximum yaw angle is presented in relation to the relative angle between wind and current. Fig. 10 shows the maximum yaw motion for the VLCC without pullback force; Fig. 11 or the Suezmax tanker.

The relative angle is always a multiple of 22.5° because of the classes defined for the wind and current directions. A relative angle equal to 0° means that either the wind and current are in line or that either the wind or current speed (or both) is equal to 0nullm/s. The size of the dots represents the probability of occurrence of that unique combination of wind, wave and current conditions. The darkness of the colour of the dots indicates that more dots overlay each other (i.e., higher probability of occurrence of that maximum yaw angle).

5.2. Pullback force is effective to reduce yaw motion

A pullback force of 800 kN generally reduces the yaw motion. Fishtailing occurs less often. Fig. 12 shows the effect pullback force on the yaw motion for the VLCC in loaded condition; Fig. 13 shows the effect for the Suezmax tanker in loaded condition. The green dots (

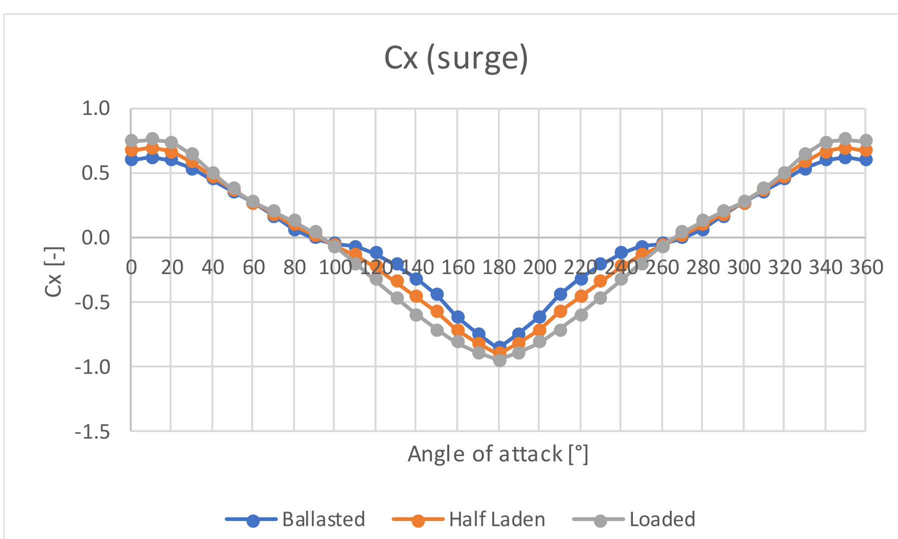

) s how the maximum yaw motion where the tanker is pulled back by 800 kN (T0800kN). The blue dots (

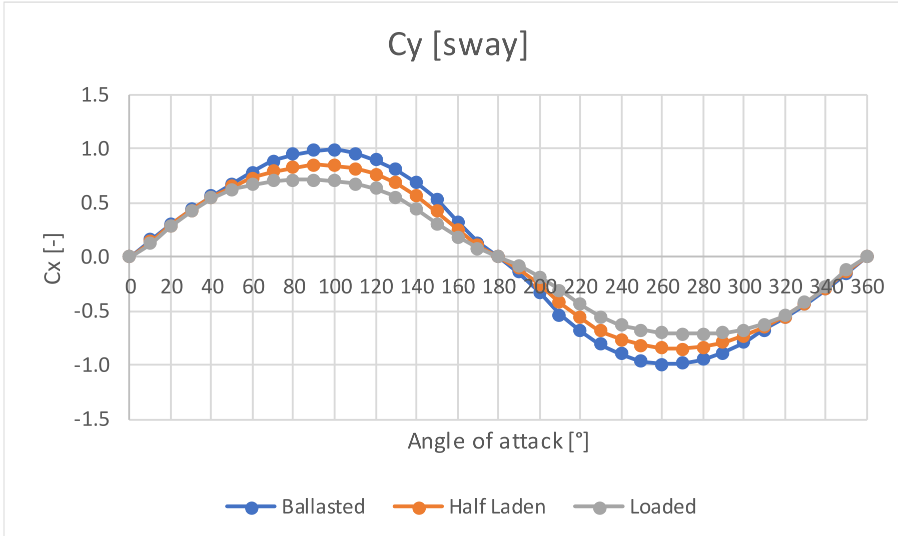

) show the maximum yaw motion without pullback force (T0000kN). Generally, a reduction of maximum yaw motion can be observed for all mooring cases.

5.3. *Pullback force effectively avoids risk of buoy kissing*

occurs when the minimum distance between the tanker and the buoy is less than 10 m (refer to Section 3a). In Figs. 14 and 15, it is evident that the pullback force that is beneath the dashed red line, occurs for both the VLCC and the Suezmax, respectively.

The pullback force (

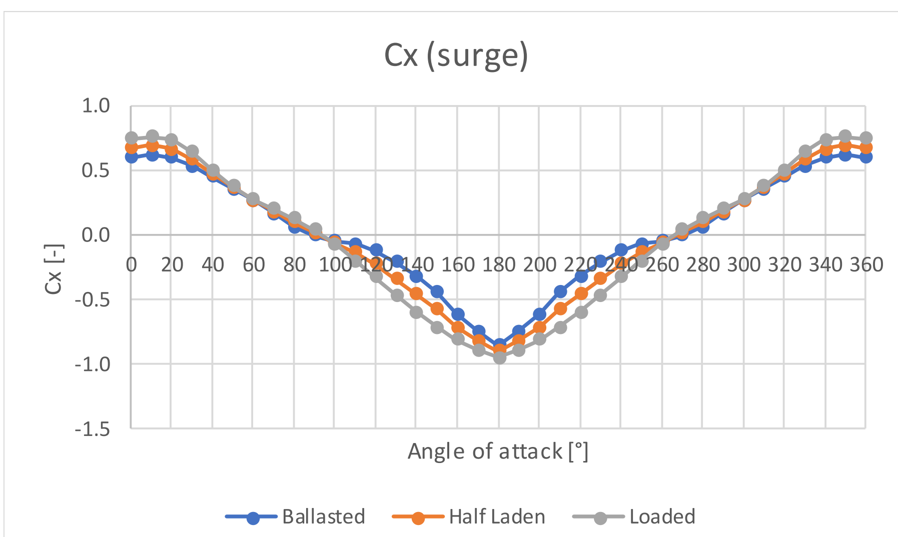

With a pullback force, buoy kissing is not likely to occur. Figs. 14 and 15 show the relation between the maximum yaw motion (fishtailing) and the minimum distance between the tanker and the buoy (buoy kissing) for respectively the VLCC and the Suezmax tanker. Buoy kissing

) effectively maintains safe distance between the tanker and the buoy (compared to no pullback force (

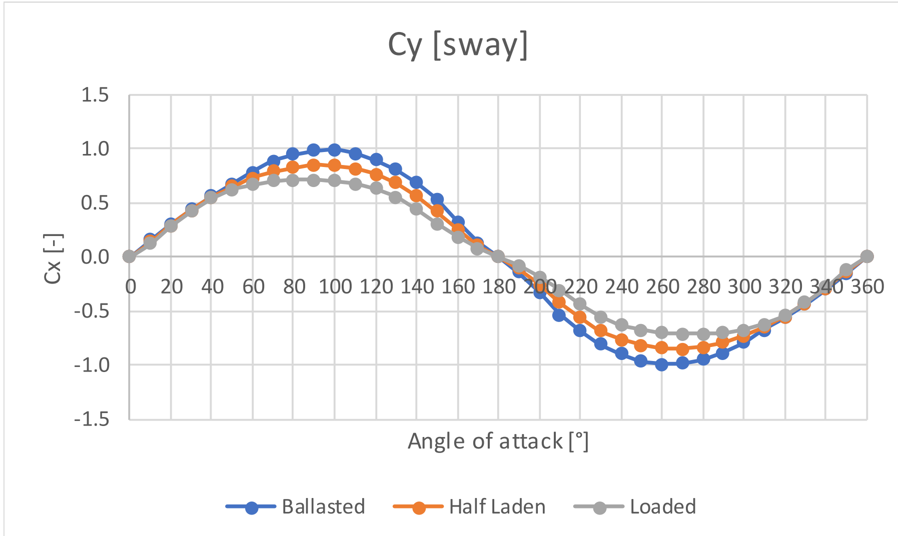

). The pullback force is therefore effective to reduce buoy kissing and fishtailing (refer to Section 4b). There are still conditions where fishtailing occurs, whether at a safe distance from the buoy (no buoy kissing). When a pullback force is applied buoy kissing does not occur when the mooring is safe. It can therefore be concluded that buoy kissing does not have to be considered for the downtime assessment.

5.4. *Capacity hawser sufficient*

The hawser line capacity is sufficient. In most conditions the hawser force is small compared to the criterion. In some conditions, fishtailing causes large mooring forces, mainly in ballasted condition. Figs. 16 and 17 show the effect on fishtailing on the maximum hawser force. When the tanker is controlled by the pullback force (

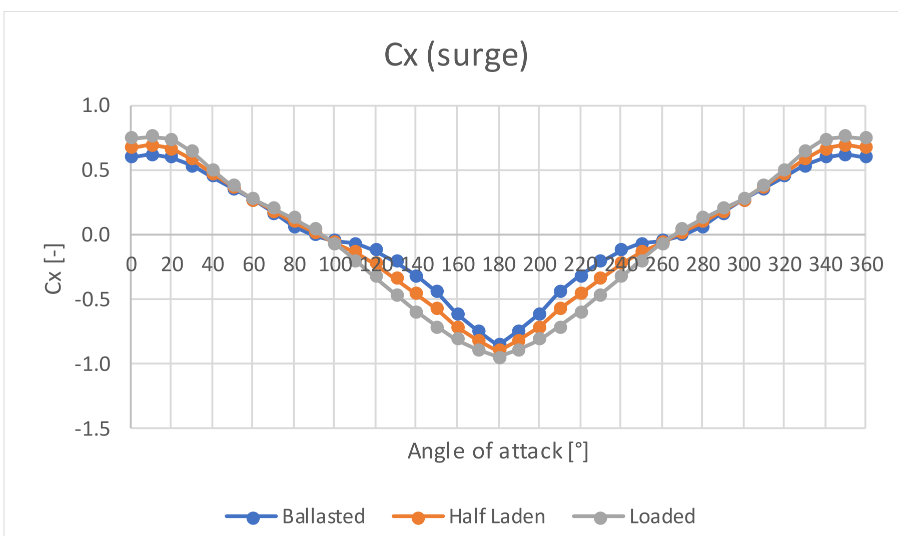

), peak loads in the hawser can be avoided. This effect is clearer in ballasted condition. If the yaw motion is not controlled (

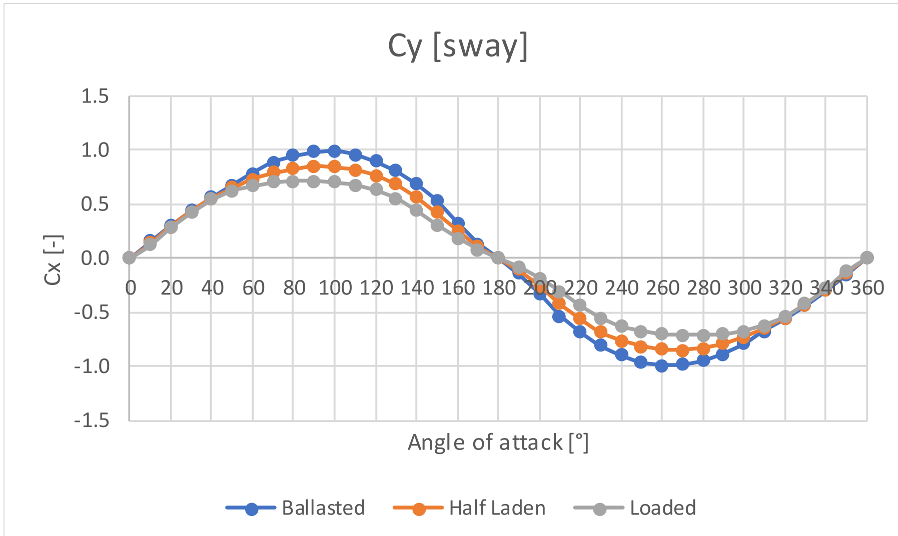

), unacceptable peak loads in the hawser occur because of the inertia of the tanker. On average though the hawser force increases because of the pullback force.

5.5. 800 kN pullback force sufficient to control tanker

A pullback force of 800 kN, in line with the tanker's centre line, effectively reduces the yaw motion (fishtailing; refer to Figs. 12 and 13) and keeps a safe distance between the tanker and the buoy (buoy kissing; refer to Figs. 14 and 15). When the yaw motion has been reduced, unacceptable peak loads in the hawser are avoided (Figs. 16 and 17). The effect of fishtailing and maximum chain force for VLCC and Suezmax showing the maximum chain forces is presented in Fig. 18.

An 800 kN pullback force in line with the tanker's centre line, representing astern propulsion and a pullback tug, significantly improves the behaviour of the moored tankers to the buoy. For CALM system, it is part of the operational procedures to have a tug on standby at all times. Particularly, it is recommended that a tug is always present while a vessel is moored to the CALM. The results demonstrate that the 800kN pullback force is sufficient to avoid fishtailing and buoy kissing. There are still some occurrences of fishtailing (without resulting in high hawser forces) but the probability of occurrence is less than 0.1%. This is considered negligibly small probability of occurrence. Furthermore, in reality the tug pulls the stern of the tanker under a more favourable angle so most likely a tug is more effective than the modelled pullback force which acts in line with the tanker. Based on this, the 70t tugs recommended are deemed to be sufficient for limiting fishtailing and buoy kissing.

6. Conclusive remarks

In this research, the CALM moored tanker system is taken as the research object, by conducting the numerical analysis on fishtailing motion, buoy kissing and pullback force. This methodology for the study

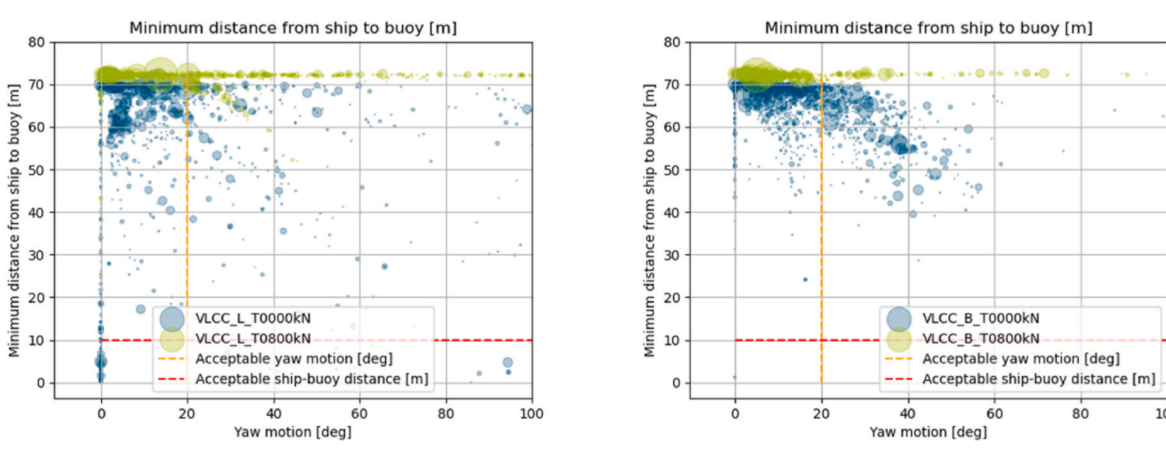

(a) VLCC loaded (b) VLCC ballasted

Fig. 14. Effect of fishtailing and pullback force on buoy kissing for VLCC.

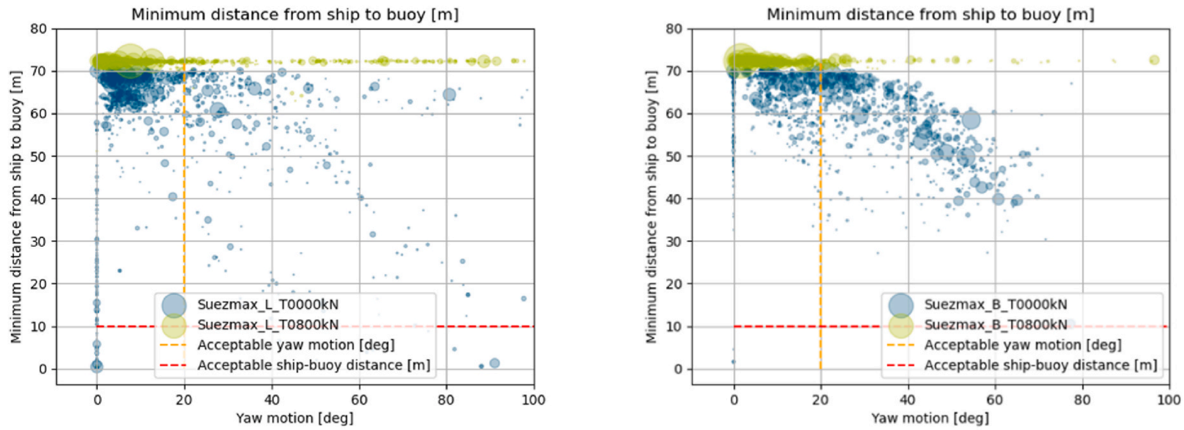

(a) Suezmax loaded (b) Suezmax ballasted

Fig. 15. Effect of fishtailing and pullback force on buoy kissing for Suezmax.

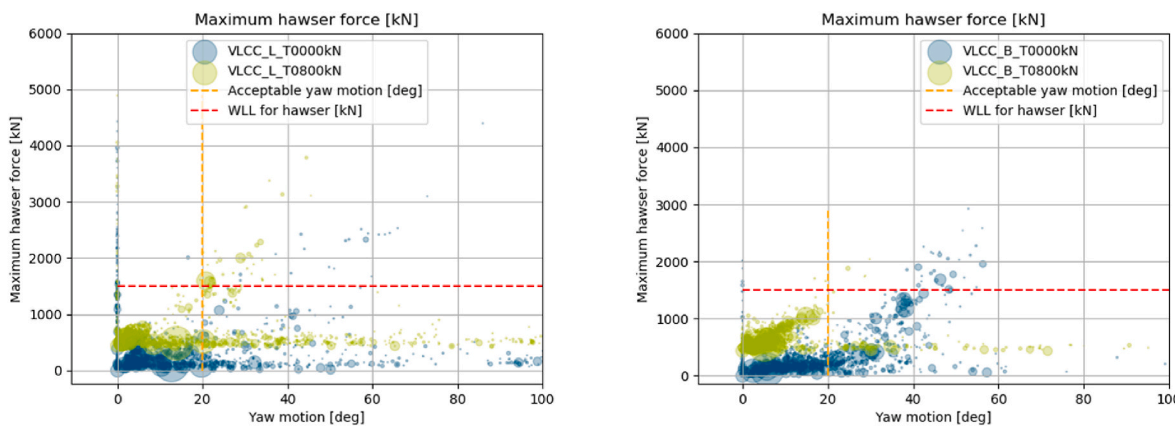

(a) VLCC loaded (b) VLCC ballasted

Fig. 16. Effect fishtailing on maximum hawser force for VLCC.

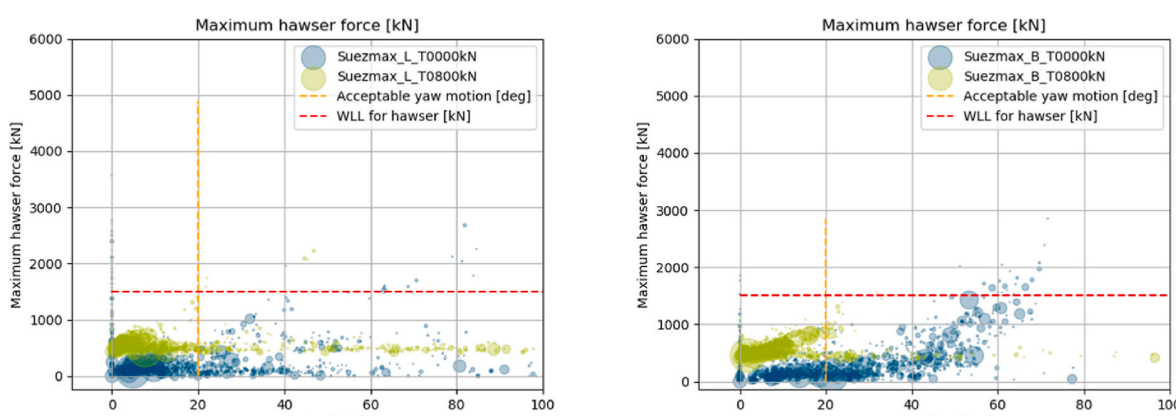

(a) Suezmax loaded (b) Suezmax ballasted

Fig. 17. Effect fishtailing on maximum hawser force for Suezmax.

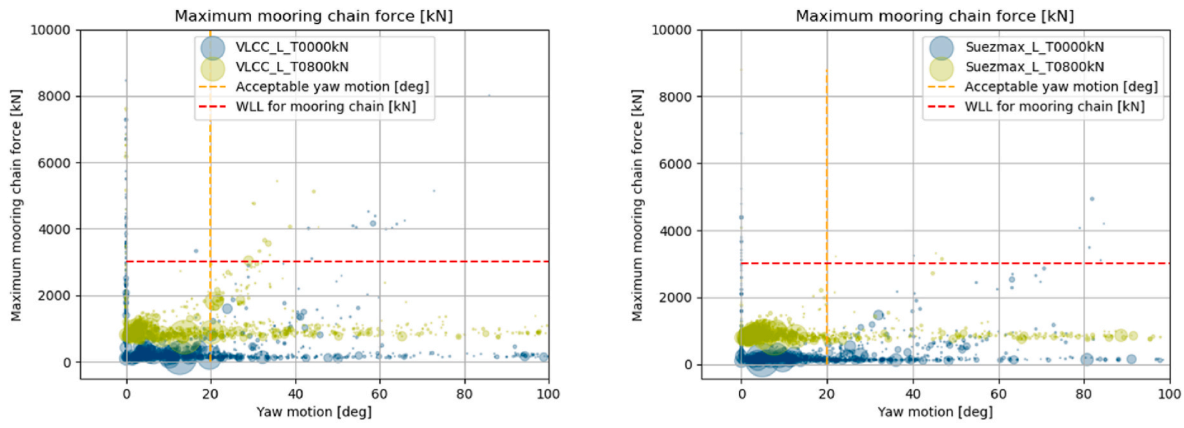

(a) VLCC loaded

(b) Suezmax loaded

Fig. 18. Effect fishtailing and maximum chain force for VLCC (left) and Suezmax (right) loaded.

includes establishing the hydrodynamic model is established and conducting a dynamic mooring analysis. The research highlights the need for stability and safety during un(loading) activities for production of oil and gas products. Also, the proposed techniques could benefit different sea states, such as Bohai Sea in China and West African Sea in offshore Nigeria, however each sea is dependent on its environmental conditions.

From this study, the following conclusions are drawn:

(1) The established model has a double-spring hydrodynamic response system model composed of "Anchoring-Buoy" and "Hawser-Tanker" for the CALM system. The method of time domain coupling simulation reveals the correlation and comprehensive analysis simulations of the fishtailing motion, buoy kissing, hawser capacity, and pullback force.
(2) Without the pullback force, fishtailing occurs often, but an 800-kN pullback force is sufficient to control VLCC and Suezmax tankers moored to the CALM system. Astern propulsion (amount decided by the tanker operator) and/or a pullback tug are required to avoid fishtailing and buoy kissing. Fishtailing generally causes large mooring forces. Buoy kissing should be prevented to avoid damage to the tanker and buoy. An 800-kN pullback force in line with the tanker's centreline, representing astern propulsion and/or a pullback tug, significantly improves the behavior of the moored tankers to the buoy. For CALM system facilities, it is part of the operational procedures to have a tug on standby at all times. In particular, it is recommended that a tug is always present while a tanker is moored to the CALM system.
(3) With regard to the hawser capacity, in most conditions the hawser force is small compared with the criterion. However, in some conditions, fishtailing causes large mooring forces, mainly in ballasted conditions. Even so, the mooring hawser is still strong enough to resist this sudden force. Therefore, it is recommended that a tug is always present while a tanker is moored to the CALM system
(4) In reality, the tug pulls the stern of the tanker to a more favourable angle, so a tug is most likely more effective than the modelled pullback force that acts in line with the tanker. Based on this, the 70-t tugs recommended for navigational purposes are deemed to be sufficient for limiting fishtailing and buoy kissing. However, further studies is recommended in the application of other transloading FSOs/FPSOs and other mooring forms to understudy buoy kissing and fishtailing under different tonnage conditions.
(5) The study shows that the mooring line and the anchors could be simplified to achieve the desired result. This provides some novelty, and the uniqueness from the simplification conducted in this modelling approach by the application of this offshore structures software – aNySIM can be utilized in further studies for other mooring systems. However, there are some shortcomings on using non-linear springs to simulate the action of anchor chains and nylon cables, which include some challenges in discretization of more complex mooring systems, and less studies have applied them in other offshore structures. As such, more coupling approaches is recommended by the use of aNySIM, with more validations should also be considered. Future work recommendations could also include risk-based analysis, integrity management and cloud based investigations for optimizing mooring systems.

Funding

This research received no external funding. However, this work was supported by High-tech Ship Research Project of Ministry of Industry and Information Technology, PRC[E-0819C002], and Science and Technology R&D Projects of China National Offshore Oil Corporation (CNOOC) [grant number CNOOC-KJ 135 JSPJ 08 GC 2019–02]. The authors also acknowledge the research support of the School of Engineering, Lancaster University, UK and the Engineering and Physical Sciences Research Council (EPSRC)'s Doctoral Training Centre (DTC), UK. The authors also recognize the support of Standards Organisation of Nigeria (SON) and the Niger Delta Development Commission (NDDC)'s Overseas Postgraduate Scholarship, both of Nigeria.

Ethical approval

It is not applicable because this article does not contain any studies with human participants or animals performed by any of the authors.

Informed consent

There is no need for informed consent as this study is not based on a questionnaire but an actual design. However, informed consent was obtained from all individual authorship participant included in the study. Also, all the images used are original to the authors, so there is no need to obtain any permission or informed consent. However, the only exceptions include Fig. 1, which was sourced from an open access publication with permission to adapt, reuse and reproduce it.Also, Figs. 4, 5 and 6 were obtained from the public domain publications of the Oil Companies International Marine Forum(OCIMF).

CRediT authorship contribution statement

Xuanze Ju: Conceptualization, Methodology, Formal analysis, Resources, Writing – original draft, preparation, Writing – review & editing, Supervision, Project administration, Funding acquisition. **Chiemela Victor Amaechi:** Conceptualization, Methodology, Validation, Writing – original draft, preparation, Writing – review & editing, Data curation, Visualization. **Baohui Dong:** Conceptualization, Methodology, Software, Validation, Formal analysis. **Xianwu Meng:** Software, Investigation, Data curation, Visualization. **Junji Li:** Methodology, Software, Formal analysis, Investigation, Data curation, Visualization.

Declaration of competing interest

The authors declare that they have no known competing financial interests or personal relationships that could have appeared to influence the work reported in this paper.

Data availability

Data will be made available on request.

Acknowledgements

This work was supported by both the High-tech Ship Research Project of Ministry of Industry and Information Technology, and the Science and Technology R&D Projects of China National Offshore Oil Corporation (CNOOC). The authors also appreciate Shell for the use of the image in Fig. 1, and also OCIMF for the images in Figs. 4, 5 and 6. The authors are greatly grateful to the journal reviewers for their helpful comments and suggestions, which help improve this paper.

Appendix

Appendix A. Wind Coefficients for both tankers

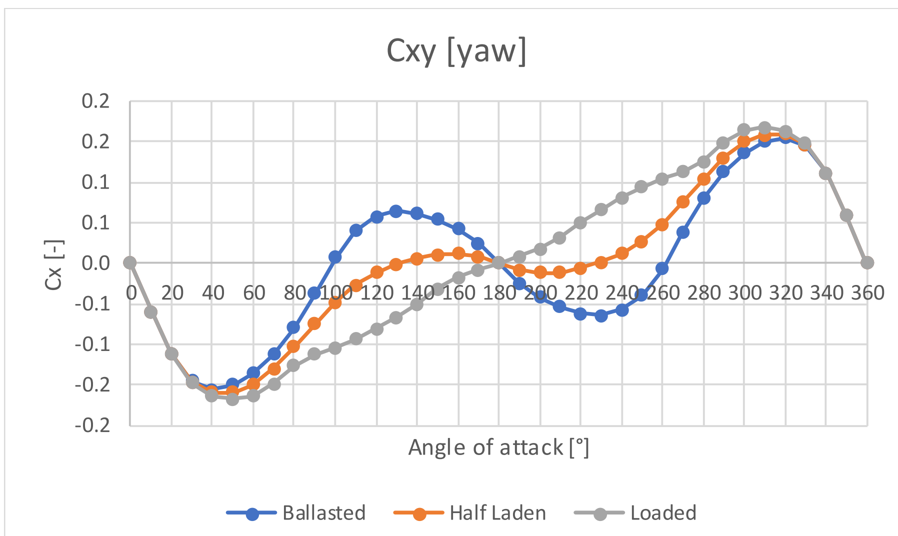

Fig. A1. Wind coefficients along surge direction for both tankers - VLCC and Suezmax.

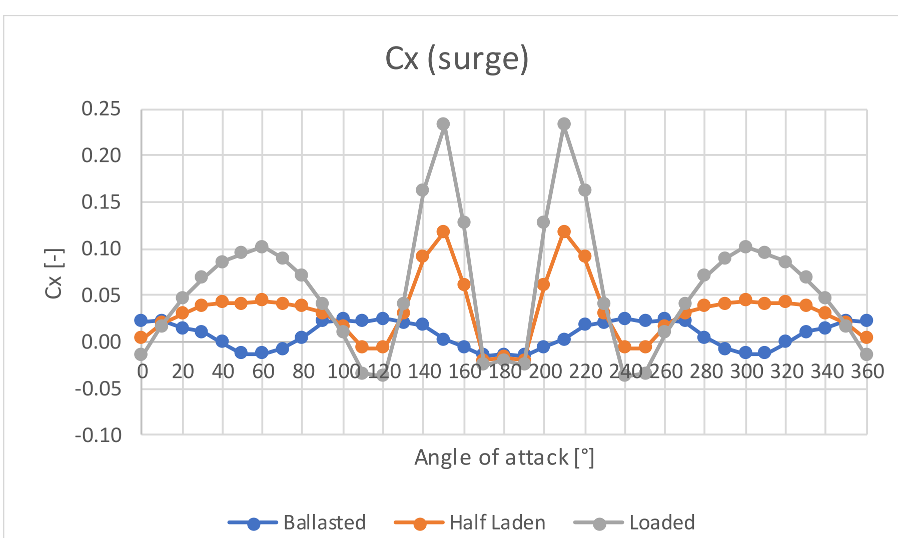

Fig. A2. Wind coefficients along sway direction for both tankers -VLCC and Suezmax.

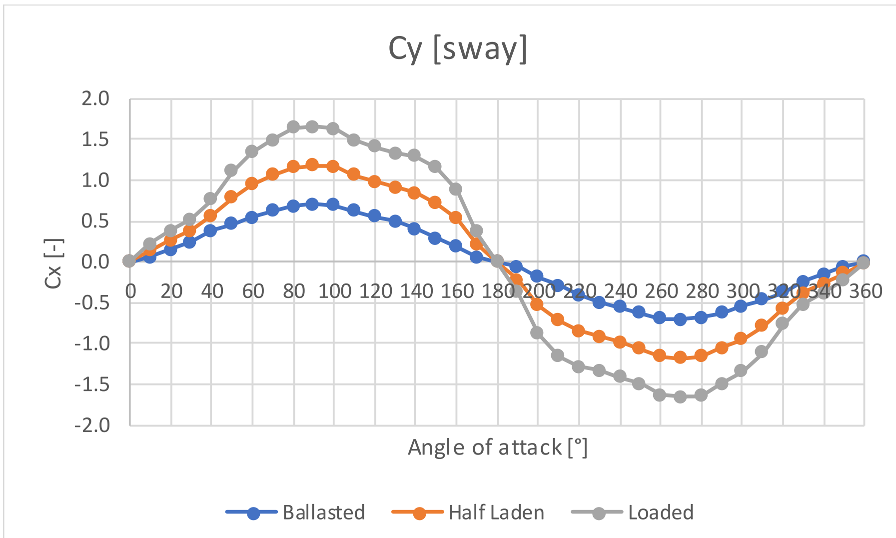

Fig. A3. Wind coefficients along yaw direction for both tankers -VLCC and Suezmax.

Appendix B. Coefficients for VLCC

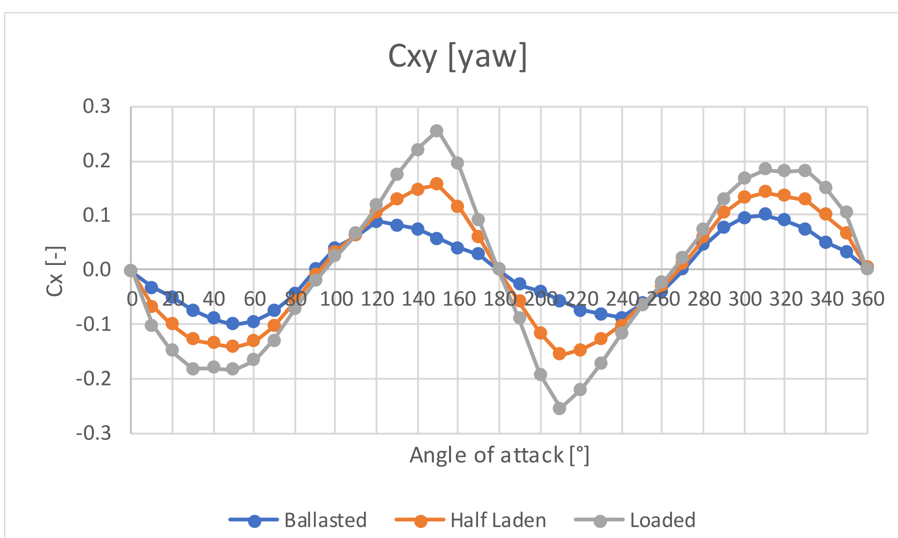

Fig. B1. Current coefficients along surge direction for VLCC.

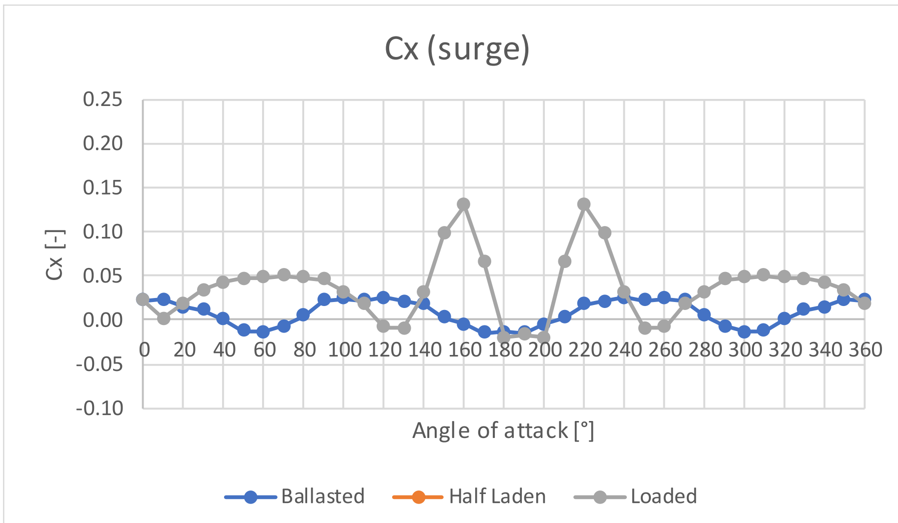

Fig. B2. Current coefficients along sway direction for VLCC.

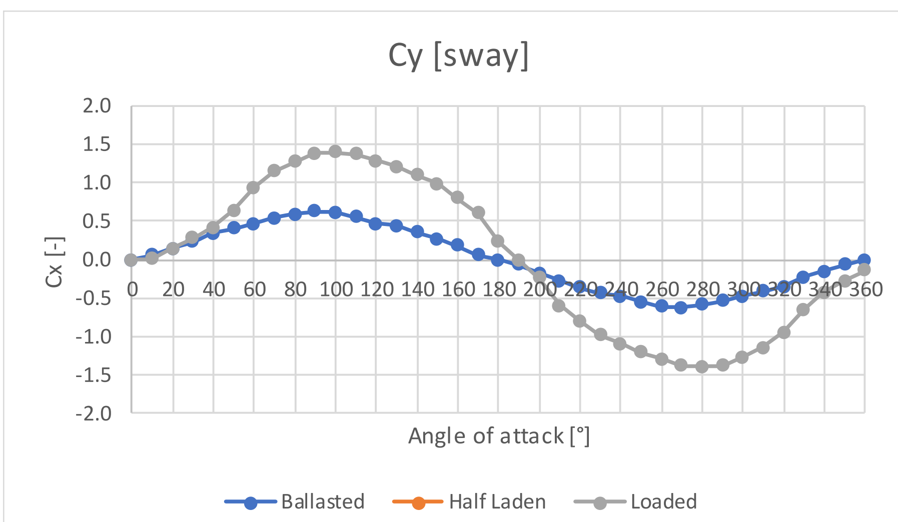

Fig. B3. Current coefficients along yaw direction for VLCC.

Appendix C. Coefficients for Suezmax

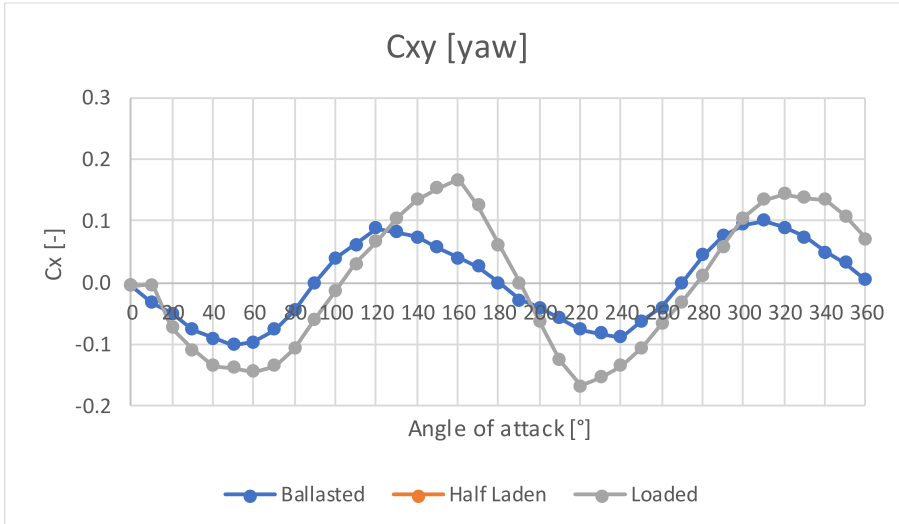

Fig. C1. Current coefficients along surge direction for Suezmax.

Fig. C2. Current coefficients along sway direction for Suezmax.

Fig. C3. Current coefficients along yaw direction for Suezmax.

References

ABS, 2022. Rules for Building and Classing—Single Point Moorings. American Bureau of Shipping, New York, NY, USA. Available at: https://ww2.eagle.org/content/dam/eagle/rules-and-guides/current/offshore/8_single_point_mooring_2022/spm-rules-july22.pdf.

Aghamohammadi, F., Thompson, J.M.T., 1990. An experimental study of the large amplitude fish-tailing instabilities of a tanker at a single point mooring. Applied ocean research 12 (1), 25–33. https://doi.org/10.1016/S0141-1187(05)80015-X.

Amaechi, C.V., Xiaonan, H., Wang, F., Ye, J., 2019. Strength of submarine hoses in Chinese-lantern configuration from hydrodynamic loads on CALM buoy. Ocean Eng. 171 (2019), 429–442. https://doi.org/10.1016/j.oceaneng.2018.11.010, 2019.

Amaechi, V.C., Wang, F., Ye, J., 2021a. Mathematical modelling of bonded marine hoses for single point mooring (SPM) systems, with catenary anchor leg mooring (CALM) buoy application—a review. J. Mar. Sci. Eng. 9 (11), 1179. https://doi.org/10.3390/jmse9111179.

Amaechi, V.C., Wang, F., Ye, J., 2021b. Numerical studies on CALM buoy motion responses and the effect of buoy geometry cum skirt dimensions with its hydrodynamic waves-current interactions. Ocean Eng. 244 (15 January 2022), 110378 https://doi.org/10.1016/j.oceaneng.2021.110378.

Asmara, I.P.S., Wibowo, V.A.P., 2020. Safety analysis of mooring hawser of FSO and SPM buoy in irregular waves. In: IOP Conference Series: Earth and Environmental Science, vol. 557. IOP Publishing, p. 12003. https://doi.org/10.1088/1755-1315/557/1/012003. No. 1.

Bai, Y., Bai, Q., 2005. Subsea Pipelines and Risers, 2013 RePrint, first ed. Elsevier, Oxford, UK.

Bernitsas, M.M., Papoulias, F.A., 1986. Stability of single point mooring systems. Appl. Ocean Res. 8 (1), 49–58. https://doi.org/10.1016/S0141-1187(86)80031-1.

Berteaux, H.O., 1976. Buoy Engineering. John Wiley and Sons, New York, NY, USA.

Brotons, M., Jean, P., 2005. Numerical vs experimental predictions of yaw motion of single point moored vessel. In: 24th International Conference on Offshore Mechanics and Arctic Engineering, Greece.

Brown, M.J., Elliot, L., 1987. A design tool for static underbuoy hose-systems. Appl. Ocean Res. 9, 171–180. https://doi.org/10.1016/0141-1187(87)90021-6.

Brown, M.J., Elliot, L., 1988. Two-dimensional dynamic analysis of a floating hose string. Appl. Ocean Res. 10 (1), 20–34. https://doi.org/10.1016/S0141-1187(88)80021-X.

Burmester, S., Vaz, G., Gueydon, S., el Moctar, O., 2020. Investigation of a semi-submersible floating wind turbine in surge decay using cfd. Ship Technol. Res. 67 (1), 2–14. https://doi.org/10.1080/09377255.2018.1555987.

Cai, Z., 2018. The legendary story of Maoming single point mooring. Sinopec Monthly (6), 94–96.

Cheng, J.J., Wang, C.J., 2017. Crude oil dock development in China: spatial distribution, capacity and problems. China Transportation Review 39 (4), 22–27.

DNVGL, 2015. DNVGL-OS-E403 Offshore Loading Buoys. Det Norske Veritas & Germanischer Lloyd, Oslo, Norway, 2015. Available at: https://rules.dnv.com/docs/pdf/DNV/os/2015-07/DNVGL-OS-E403.pdf.

DNVGL, 2020. DNVGL-OS-E403 Offshore Loading Units. Det Norske Veritas & Germanischer Lloyd, : Oslo, Norway, 2020. Available at: https://rules.dnv.com/docs/pdf/DNV/OS/2020-07/DNVGL-OS-E403.pdf.

Edward, C., Dev, A.K., 2020. Assessment of CALM buoys motion response and dominant OPB/IPB inducing parameters on fatigue failure of offshore mooring chains. In: Practical Design of Ships and Other Floating Structures, Proceedings of PRADS 2009 Conference, 64. Lecture Notes in Civil Engineering; Springer International Publishing: Berlin/Heidelberg, Germany, pp. 548–579. https://doi.org/10.1007/978-981-15-4672-3_35.

Eedalat, P., Hasanvand, E., 2021. Mooring system fatigue analysis for CALM and SALM oil terminals. International Journal of Maritime Technology - ijmt 15, 51–65. URL: http://ijmt.ir/article-1-741-en.html.

Eskilsson, C., Palm, J., 2022. High-fidelity modelling of moored marine structures: multi-component simulations and fluid-mooring coupling. J. Ocean Eng. Mar. Energy 8, 513–526. https://doi.org/10.1007/s40722-022-00263-w.

Esmailzadeh, E., Goodarzi, A., 2001. Stability analysis of a CALM floating offshore structure. Int. J. Non Lin. Mech. 36 (6), 917–926. https://doi.org/10.1016/S0020-7462(00)00055-X.

Fang, H.C., Xu, X.P., 1989. Sea wave motion response of a single point moored tanker floating production system. Acta Petolei Sinica (4), 114–121.

Ge, S., Pan, X.R., Wang, D.J., et al., 2022. Stability analysis of single point mooring and countermeasures of fishtailing oscillations[J]. Ship Science and Technology 44 (2), 70–77.

Gu, M., 2006. Safety Assessment of VLCC unloading in maoming single point mooring system. Safety Environment Health (6), 15–19.

Gueydon, S., 2016. Aerodynamic damping on a semisubmersible floating foundation for wind turbines. Energy Proc. 94 (September 2016), 367–378. https://doi.org/10.1016/j.egypro.2016.09.196.

Gueydon, S., Lindenburg, K., Savenije, F., 2013. Coupling of two tools for the simulation of floating wind turbines. In: Proceedings of the ASME 2013 32nd International Conference on Ocean, Offshore and Arctic Engineering, vol. 8. Ocean Renewable Energy, Nantes, France. https://doi.org/10.1115/OMAE2013-11174. June 9–14, 2013. V008T09A073. ASME.

Gueydon, S., Duarte, T., Jonkman, J., Bayati, I., Sarmento, A., 2014. Comparison of Second-Order Loads on a Semisubmersible Floating Wind Turbine. 33rd International Conference on Ocean. Offshore & Arctic Engineering, San Francisco (CA. https://doi.org/10.1115/OMAE2014-23398. Available at: (Accessed 17 February 2023) https://www.nrel.gov/docs/fy14osti/61162.pdf.

Halliwell, A.R., Harris, R.E., 1988. A parametric experimental study of low frequency motion of single point mooring systems in waves. Appl. Ocean Res. 10 (2), 74–86.

Hasanvand, E., Edalat, P., 2020. Sensitivity analysis of the dynamic response of CALM oil terminal, in the Persian gulf region under different operation parameters. Mar. Eng. 16 (32), 73–84 (in Persian). URL: http://marine-eng.ir/article-1-794-en.html.
Hasanvand, E., Edalat, P., 2021a. Evaluation of the safe and failure zones of mooring and riser systems in a CALM oil terminal. J. Mar. Sci. Appl. 20, 751–766. https://doi.org/10.1007/s11804-021-00240-z.
Hasanvand, E., Edalat, P., 2021b. A comparison of the dynamic response of a product transfer system in CALM and SALM oil terminals in operational and non-operational modes in the Persian gulf region. Int. J. Coast. Offshore Eng. 5, 1–14.
Hasanvand, E., Edalat, P., 2021c. Comparison of dynamic response of Chinese lantern and Lazy S riser configurations used in CALM oil terminal. Journal Of Marine Engineering 17 (33), 37–52 (in Persian). URL: http://marine-eng.ir/files/site1/user_files_13d531/edalat-A-10-627-3-12b2111.pdf.
Hengyi Brunei PMB petrochemical project ushered in the first shipment of crude oil, large quantities of materials have entered. Retrieved May 5, 2019, from. http://www.hengyi.com/news/html/?836.html.
Hollister, H.D., Spokes, J.J., 2004. The Agbami Project: a World Class Deepwater development[C]. Offshore Technology Conference, Houston.
Hollyhead, C.J., Townsend, N.C., Blake, J.I., 2017. Experimental investigations into the current-induced motion of a lifeboat at a single point mooring. Ocean Eng. 146, 192–201. https://doi.org/10.1016/j.oceaneng.2017.09.045.
Huang, G.L., Fujino, M., 1987. Fishtailing oscillation of a ship moored to single point mooring systems in wind and current. Ocean Eng. (3), 1–13.
Huo, Ping, Wang, Dongjiao, Kun, Liu, 2018. Research on fishtailing oscillations of a single point moored vessel in shallow waters. In: Paper Presented at the the 28th International Ocean and Polar Engineering Conference. Sapporo, Japan. Available at: https://onepetro.org/ISOPEIOPEC/proceedings-abstract/ISOPE18/All-ISOPE18/ISOPE-I-18-186/20426. (Accessed 17 February 2023) http://publications.isope.org/proceedings/ISOPE/ISOPE%202018/data/polopoly_fs/1.4192175.1525883485!/fileserver/file/893334/filename/18TPC-0290Huo.pdf.
Ja'e, I.A., Ali, M.O.A., Yenduri, A., Nizamani, Z., Nakayama, A., 2022. Effect of various mooring materials on hydrodynamic responses of turret-moored FPSO with emphasis on intact and damaged conditions. J. Mar. Sci. Eng. 10 (4), 453. https://doi.org/10.3390/jmse10040453.
Ji, C.Q., 2000. Influence of various parameters on mooring motion and load of single point. China Offshore Platform 15 (1), 19–23.
Ji, C.X., Chen, S.C., Xie, H.B., 2014. Feasible degree research of navigation environment for CALM type single point mooring system. J. Dalian Marit. Univ. 40 (2), 34–38.
Jin, Y., Xie, K., Liu, G., Peng, Y., Wan, B., 2022. Nonlinear dynamics modeling and analysis of a marine buoy single-point mooring system. Ocean Eng. 262, 112031 https://doi.org/10.1016/j.oceaneng.2022.112031.
Ju, X., Li, Z., Dong, B., Meng, X., Huang, S., 2022a. Mathematical physics modelling and prediction of oil spill trajectory for a catenary anchor leg mooring (CALM) system. Advances in Mathematical Physics 2022. https://doi.org/10.1155/2022/3909552.
Ju, Xuanze, Li, Zili, Dong, Baohui, Wang, Jianghong, Meng, Xianwu, 2022b. Engineering Investigation of a Deepwater Turret Mooring Suction Pile Inverse Catenary Based on BV and DNVGL Rules. July-August 2022, ahead-of print. Forest Chemicals Review, pp. 788–802. Available at: http://www.forestchemicalsreview.com/index.php/JFCR/article/view/966.
Lee, Sang-Won, Kim, Young-Du, 2019. A study on improvement of criteria for mooring safety assessment in single point mooring. Journal of the Korean Society of Marine Environment and Safety 25 (3), 287–297. https://doi.org/10.7837/kosomes.2019.25.3.287.
Li, Y.Z., Liu, F.S., 2019. Fishtail motion of tanker moored to CALM system. Guangdong Shipbuilding 38 (6), 21–23.
Liang, W.W., Li, Z.Y., Ma, J., 2019. Study on construction scale of large crude oil wharf in Dongying Port area. Shandong Communication Science and Technology (4), 27–29.
Lu, Y., Ju, X., Li, X., Li, G., Dong, B., Zhong, C., 2018. Construction conditions and site selection of catenary anchor leg mooring CALM) for offshore oil terminal. Ocean Engineering Equipment and Technology 5 (5). https://doi.org/10.12087/oeet.2095-7297.2018.05.02 (in Chinese).
Lv, Y., Ju, X.Z., et al., 2018. Study on construction conditions & site selection of catenary anchor leg mooring (CALM) for offshore oil terminal. Ocean Engineering Equipment and Technology 5 (5), 300–304.
Ma, S., Kim, M.H., Shi, S., 2009. Second-order low-frequency wave forces on a SPM offloading tanker in shallow water. J. Offshore Mech. Arctic Eng. 131 (4), 901–908.
Maari, R., 1985. Single Point Mooring. Principality of Monaco.
MARIN, 2022. aNySIM Software. MARIN. Maritime Research Institute Netherlands), Wageningen, The Netherlands. Available at: https://www.marin.nl/en/facilities-and-tools/software/anysim. (Accessed 17 February 2023).
OCIMF, 2009. Guide to manufacturing and purchasing hoses for offshore moorings (GMPHOM). In: Oil Companies International Marine Forum (OCIMF), fifth ed. Witherby & Co., London, UK. 2009.
OCIMF, 2015. Single point mooring maintenance and operations guide. In: Oil Companies International Marine Forum(OCIMF), third ed. Witherby & Co., London, UK. 2015.
OCIMF, 2018. Mooring equipment guidelines (MEG4). In: Oil Companies International Marine Forum (OCIMF), fourth ed. Witherby & Co., London, UK. 2018.
Pecher, A., Foglia, A., Kofoed, J.P., 2014. Comparison and sensitivity investigations of a CALM and SALM Type mooring system for wave energy converters. J. Mar. Sci. Eng. 2 (1), 93–122. https://doi.org/10.3390/jmse2010093.
Rutkowski, G., 2019a. A comparison between conventional buoy mooring CBM, single point mooring SPM and single anchor loading SAL systems considering the hydro-meteorological condition limits for safe ship's operation offshore. *TransNav, the International Journal on Marine Navigation and Safety of Sea Transportation* 13 (1), 187–195. https://doi.org/10.12716/1001.13.01.19, 2019.
Rutkowski, G., 2019b. A comparison between DP offshore loading operation on submerged turret loading system STL, submerged single anchor loading system SAL and offshore loading system OLS considering the hydro-meteorological condition limits for the safe ship's operation offshore. *TransNav, the International Journal on Marine Navigation and Safety of Sea Transportation* 13 (1), 175–185. https://doi.org/10.12716/1001.13.01.18.
Ryu, S., Duggal, A.S., Heyl, C.N., et al., 2006. Prediction of deepwater oil offloading buoy response and experimental validation. Int. J. Offshore Polar Eng. 16 (4), 290–296.
Schellin, T.E., 2003. Mooring load of a ship single-point moored in a steady current. Mar. Struct. 16 (2), 135–148.
Shell DEP 37.91.10.10-Gen, Single Point Mooring System, 2011.
Simos, A.N., Tannuri, E.A., Aranha, J.A.P., et al., 2001a. Theoretical analysis and experimental evaluation of the fishtailing phenomenon in a single-point moored tanker. In: Proceedings of the Eleventh (2001) International Offshore and Polar Engineering Conference. Norway.
Simos, Alexandre N., Tannuri, Eduardo A., Aranha, José A.P., André, J.P., Leite, 2001b. Theoretical analysis and experimental evaluation of the fishtailing phenomenon in a single-point moored tanker. Stavanger, Norway. In: Paper Presented at the the Eleventh International Offshore and Polar Engineering Conference. Available at: https://www.researchgate.net/publication/268424637_Theoretical_Analysis_and_Experimental_Evaluation_of_the_Fishtailing_Phenomenon_in_a_Single-Point_Moored_Tanker. (Accessed 17 February 2023).
Sun, C.Q., Zhu, Z.Q., Geng, X.W., 1988. Wave tests of a single buoy store system model. Ocean Eng. 6 (1), 89–95.
Sun, Q., Peng, G.S., Dong, Q.H., 2014. Design and analysis method research on CALM type single point mooring system. In: The 16th Annual Conference of China Association for Science and Technology— Symposium on Green Shipbuilding and Safe Shipping, pp. 126–131.
Tannuri, E.A., Simos, A.N., Leite, A.J.P., Aranha, J.A.P., 2001. Experimental validation of a quasi-explicit hydrodynamic model: fishtailing instability of a single-point moored tanker in rigid-hawser configuration. J. Ship Res. 45, 302–314. https://doi.org/10.5957/jsr.2001.45.4.302. Available at: (Accessed 17 February 2023) https://www.researchgate.net/publication/233682281_Experimental_Validation_of_a_Quasi-Explicit_Hydrodynamic_Model_Fishtailing_Instability_of_a_Single-Point_Moored_Tanker_in_Rigid-Hawser_Configuration.
van den Berg, J., Pauw, W.H., 2018. aNySIM Theory Documentation. Maritime Research Institute Netherlands (MARIN), Wageningen.
Weller, S., Gueydon, S., 2012. Analysis of the DeepCwind Model Tests and a First Attempt to Simulate a Semi-submersible Floating Wind Platform with aNySIM. MARIN, Wageningen, The Netherlands. https://doi.org/10.13140/RG.2.2.14465.56168. Technical Report No. 24602-MSG-1.
Wichers, J.E.W., 1988. A Simulation Model for a Single Point Moored Tanker. Delft University of Technology, The Netherlands.
Wichers, I.J., 2013. Guide to Single Point Moorings. WMooring Inc, Houston, TX, USA. Available online: http://www.wmooring.com/files/Guide_to_Single_Point_Moorings.pdf. (Accessed 17 February 2023).
Wu, L.K., 2004. On the contrast of the merit and shortness for single point mooring terminal and fixed oil quay[J]. China Offshore Platform 20 (1), 39–41.
Xu, X.P., Tong, Y.Y., 1994. Dynamic response analysis of single point mooring system. Journal of China University of Petroleum(Edition of Natural Science) (5), 74–78.
Yang, Ray-Yeng, Chiang, Wen-Chang, 2022a. Dynamic Motion Response of an Oil Tanker Moored with a Single Buoy under Different Mooring System Failure Scenarios. Ships and Offshore Structures. https://doi.org/10.1080/17445302.2022.2082105 ahead-of print.
Yang, R.Y., Chiang, W.C., 2022b. Dynamic motion response of an oil tanker moored with a single buoy under different mooring system failure scenarios. Ships Offshore Struct. 1–14. https://doi.org/10.1080/17445302.2022.2082105.
Yu, J.X., Wang, Y.G., Wang, H.W., 2005. The force analysis of a ship single point moored under the combined action of wind, wave and tide[J]. Ocean Technology 24 (3), 96–100.
Yu, J., Ding, H., Yu, Y., Wu, S., Zeng, Q., Ma, W., 2022. A novel risk analysis approach for FPSO single point mooring system using Bayesian Network and interval type-2 fuzzy sets. Ocean Eng. 266, 113144 https://doi.org/10.1016/j.oceaneng.2022.113144.
Yu, J., Zeng, Q., Yu, Y., Wu, S., Ding, H., Ma, W., et al., 2023. Failure mode and effects analysis based on rough cloud model and MULTIMOORA method: application to single-point mooring system. Appl. Soft Comput. 132, 109841 https://doi.org/10.1016/j.asoc.2022.109841.
Zhang, X.M., Li, W.Y., 1988. The motions and mooring loads of a spy system due to wind, current and waves. Ocean Eng. (4), 17–28.
Zhang, L., Yang, J.M., Lv, H.N., et al., 2012. Investigation on hydrodynamic performances of deepwater CALM buoy and shuttle tanker off West Africa. Ocean Eng. 30 (3), 9–17.
Zhang, X., Ni, W., Sun, L., Zhang, W., 2021. Experimental investigation of a shuttle tanker in irregular waves with hawser single point mooring system. Ships Offshore Struct. 16 (8), 838–851. https://doi.org/10.1080/17445302.2020.1786236.
Zhou, N., 2018. Fish-tailing effect of a tanker moored to a CALM SPM system. China Offshore Platform 33 (5), 70–74.
Zhou, N., Dong, B.H., Li, J.J., et al., 2020. Key points in design of calm single point mooring facilities. Ocean Engineering Equipment and Technology 7 (6), 425–429.
Ziccardi, J.J., Robbins, H.J., 1970. Selection of hose systems for SPM tanker terminals. In: Offshore Technology Conference Proceeding. Publisher: OnePetro, Texas, USA, pp. 83–94. https://doi.org/10.4043/1152-ms.